THE HEAT CONDUCTIVITY OF POLYATOMIC GASES IN MAGNETIC FIELDS

L. J. F. HERMANS

THE HEAT CONDUCTIVITY OF POLYATOMIC GASES IN MAGNETIC FIELDS

THE HEAT CONDUCTIVITY OF POLYATOMIC GASES IN MAGNETIC FIELDS

PROEFSCHRIFT

TER VERKRIJGING VAN DE GRAAD VAN DOCTOR
IN DE WISKUNDE EN NATUURWETENSCHAPPEN AAN DE
RIJKSUNIVERSITEIT TE LEIDEN,
OP GEZAG VAN DE RECTOR MAGNIFICUS DR. J. GOSLINGS,
HOOGLERAAR IN DE FACULTEIT DER GENEESKUNDE,
TEN OVERSTAAN VAN EEN COMMISSIE UIT DE SENAAT
TE VERDEDIGEN OP DONDERDAG 18 JUNI 1970
TE KLOKKE 15.15 UUR

DOOR

LODEWIJK JOZEF FREDERIK HERMANS
GEBOREN TE KERKRADE IN 1937

1970
KONINKLIJKE DRUKKERIJ VAN DE GARDE N.V.
ZALTBOMMEL

Promotor: PROF. DR. C. J. GORTER

Dit proefschrift is tot stand gekomen onder leiding van

PROF. DR. J. J. M. BEENAKKER en DR. H. F. P. KNAAP

STELLINGEN

I

De verhouding van de warmtegeleidingscoëfficiënten van waterstof en deuterium bij 300 K is aanzienlijk beter in overeenstemming met de theorie, dan de literatuurwaarden suggereren.

Hoofdstuk III van dit proefschrift.

II

Door een incorrecte toepassing van de tweede wet van Kirchhoff is de beschrijving, die Wipf geeft van het gedrag van een wisselstroom door een supergeleider van de tweede soort in een magnetisch veld, onjuist.

Wipf, S. L., Proc. 1968 Summer Study on Superconducting Devices and Accelerators, Part II (BNL 50155 (C-55)) p. 514.

III

Voor regelmatig terugkerende berekeningen op een computer verdient inbrengen op afstand van het programma (remote job entry) de voorkeur boven het zogenaamde conversationele werken op een terminal.

IV

De bewering van Dông en Durup, dat de botsingsdoorsnede voor de door botsing geïnduceerde dissociatie van HeH^+ in eerste orde Born-benadering een even functie is van de cosinus van de afbuigingshoek, is onjuist.

Dông, P. en Durup, J., Chem. Phys. Letters **5** (1970) 340.
Schopman, J. en Los, J., Phys. Letters **31A** (1970) 79.

V

Bij metingen van absolute lichtintensiteiten met behulp van kegelvormige detectoren wordt veelal onvoldoende aandacht geschonken aan de oriëntatie van de detector ten opzichte van de lichtbundel.

Eisenman, W. L., Bates, R. L. en Merriam, J. D., J. Opt. Soc. Am. **53** (1963) 729.

VI

Bij het meten van de warmtegeleiding in sterk magnetische kristallen bij lage temperaturen treden zeer lange insteltijden op. Dit kan tot onjuiste interpretatie van anomale resultaten leiden.

Rao, K. V., Phys. Rev. Letters **22** (1969) 943.
Anderson, A. C. en Malinowski, M. E., Phys. Status Solidi **37** (1970) K 141.

VII

Bij de interpretatie van het spectrum van aan CO_2-gas verstrooid licht houden Greytak en Benedek ten onrechte geen rekening met het feit, dat een aanzienlijk deel van de intensiteit afkomstig is van het anisotrope deel van de polariseerbaarheid.

Greytak, T. J. en Benedek, G. B., Phys. Rev. Letters **17** (1966) 179.

VIII

Het op theoretische gronden verwachte verband tussen transversale (λ^{tr}) en longitudinale ($\Delta\lambda^{//}$, $\Delta\lambda^{\perp}$) warmtegeleidingscoëfficiënten van gassen in magnetische velden wordt voor een aantal eenvoudige gassen inderdaad gevonden.

Tip, A., Levi, A. C. en McCourt, F. R., Physica **40** (1968) 435.
Hermans, L. J. F. en Heemskerk, J. P. J., te publiceren in Physica.

IX

Voor het meten van warmtegeleidingscoëfficiënten van gassen biedt een apparaat van het type, dat gebruikt wordt voor het meten van veranderingen van de warmtegeleiding in een magnetisch veld, enige voordelen boven de gangbare technieken.

Hoofdstuk III van dit proefschrift.

X

Op zomerse weekeinden wordt de maximale capaciteit van de Nederlandse autowegen bereikt bij een verkeerssnelheid van ongeveer 24 km/uur, indien de verkeersdeelnemers op de voorgeschreven wijze afstand houden.

Aan mijn ouders
Aan mijn gezin

Het in dit proefschrift beschreven onderzoek werd uitgevoerd als onderdeel van het programma van de Werkgemeenschap voor Molecuulphysica van de Stichting voor Fundamenteel Onderzoek der Materie (F.O.M.) met financiële steun van de Nederlandse Organisatie voor Zuiver Wetenschappelijk Onderzoek (Z.W.O.).

CONTENTS

INTRODUCTION

In 1930 it was found by Senftleben[1]) that the thermal conductivity of gaseous O_2 and NO decreases slightly under the influence of a magnetic field. This phenomenon can be explained on the basis of the mean free path theory, as was first shown by Gorter in 1938[2]) in the following way. The collision probability of a non-spherical molecule depends on its orientation with respect to the flight direction. Since paramagnetic molecules like O_2 and NO have a magnetic moment coupled to the axis of rotation, they will in the presence of a magnetic field carry out a precession around the field direction during the free flight time between two collisions. This will result in an averaging of the mean collision probability, and thus in a change in the mean free path, when the precession frequency is sufficiently large with respect to the collision frequency. Since the mean free path determines the heat conductivity and the viscosity, these transport properties can also be expected to be influenced by magnetic fields. It is clear from this picture that these changes are a function of the ratio of precession frequency, ω_p, and collision frequency, ω_c, and that the effects will reach a saturation value for

$$1 \ll \frac{\omega_p}{\omega_c} \propto \frac{H\mu}{p}, \tag{1}$$

where H is the magnetic field strength, p is the pressure and μ is the magnetic moment along the axis of rotation, which is, for paramagnetic gases, of the order of a Bohr magneton. Indeed, it was found experimentally that these phenomena can be described as a function of H/p.

During the 1930's, no effects were observed for non-paramagnetic gases, suggesting that the above mentioned phenomena were exclusive properties of paramagnetic gases. However, in 1962 it was experimentally demonstrated

by Beenakker *et al.*[3]) that also diamagnetic gases (*e.g.* N_2) are influenced by a magnetic field. In this case the field acts on the magnetic moment which is caused by the rotation of the molecules. This magnetic moment is of the order of a nuclear magneton and can be written as

$$\boldsymbol{\mu} = g\mu_N \boldsymbol{J}, \tag{2}$$

where μ_N is the nuclear magneton, $\boldsymbol{J}$ is the angular momentum in units $\hbar$ and g is the rotational Landé-factor, which can be positive or negative†. Because this magnetic moment is extremely small, higher fields and lower pressures are necessary in order to obtain values of $\omega_p/\omega_c \gtrsim 1$. The relative change in the transport properties, however, will at saturation be of the same order of magnitude as was found for paramagnetic gases (*i.e.*, of the order 10^{-2}), since it is connected to the non-sphericity of the molecules.

The experiments described in this thesis deal with heat conductivity in a magnetic field. Fourier's law for heat conduction in an anisotropic medium can be written as

$$q_i = -\sum_k \lambda_{ik} \frac{\partial T}{\partial x_k}, \tag{3}$$

indicating that heat transport in the i-direction can be caused by a temperature gradient in any direction. It was shown by De Groot and Mazur[4]) in 1963, using symmetry arguments, that, for an isotropic medium placed in a magnetic field, eq. (3) reduces to

$$\begin{Bmatrix} q_x \\ q_y \\ q_z \end{Bmatrix} = - \begin{bmatrix} \lambda^{//} & 0 & 0 \\ 0 & \lambda^{\perp} & -\lambda^{tr} \\ 0 & \lambda^{tr} & \lambda^{\perp} \end{bmatrix} \begin{Bmatrix} \frac{\partial T}{\partial x} \\ \frac{\partial T}{\partial y} \\ \frac{\partial T}{\partial z} \end{Bmatrix} \tag{4}$$

when the magnetic field is chosen along the x-axis. The significance of the tensor elements $\lambda^{//}$, $\lambda^{\perp}$ and λ^{tr} is illustrated in fig. 1. The diagonal elements denote the heat conduction parallel to an applied temperature gradient, in the presence of a magnetic field parallel to the gradient ($\lambda^{//}$) or perpendicular to the gradient ($\lambda^{\perp}$), while λ^{tr} corresponds to transverse heat flow perpendicular to both applied temperature gradient and magnetic field. (Such transverse heat transport had been known in metals for a long time under the name Righi–Leduc effect). In the absence of a field, $\lambda^{//} = \lambda^{\perp} = \lambda_0$

† It should be noted, that even in weak magnetic fields the nuclear spin magnetic moment (if present) is decoupled from the rotational magnetic moment. Thus, the nuclear spin does not ordinarily play a role in these effects.

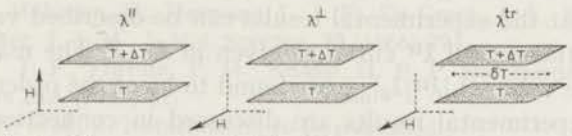

Fig. 1. The experimental significance of $\lambda^{//}$, $\lambda^{\perp}$ and λ^{tr}.

and $\lambda^{tr} = 0$. The quantities $\lambda^{//}$ and $\lambda^{\perp}$ are analogous to magnetoresistance in electrical conduction, while λ^{tr} is analogous to the Hall coefficient. As in the electrical case, $\Delta\lambda^{//}$ $(= \lambda^{//} - \lambda_0)$ and $\Delta\lambda^{\perp}(= \lambda^{\perp} - \lambda_0)$ are even functions of the field, while λ^{tr} is an odd function of the field.

In the 1960's, the theory for the Senftleben–Beenakker effect was developed along the lines of the Chapman–Enskog theory. In the course of these calculations, it was proven independently by Knaap and Beenakker[5]), Kagan and Maksimov[6]) and McCourt and Snider[7]) that λ^{tr} should be non-zero for polyatomic gases in a magnetic field. The theoretical field dependence of $\Delta\lambda^{//}$, $\Delta\lambda^{\perp}$ and λ^{tr} as found by these authors is shown in fig. 2.

After the theoretical prediction that for polyatomic gases transverse heat transport should exist, we experimentally verified that indeed $\lambda^{tr} \neq 0$ for O_2, N_2, HD and CO_2, shortly (in fact 2 days!) after Korving had verified the existence of transverse effects in the viscosity. Since these transverse effects are odd in g (see eqs. (1) and (2)), the sign of g for these gases was determined from both experiments and published in a note[8]). The accuracy in these early λ^{tr} experiments at room temperature was, however, very poor due to large radiative heat losses. Therefore, an apparatus was designed for measuring at lower temperatures. At 85 K reliable values of λ^{tr} were obtained and reported as preliminary results in a letter[9]).

In chapter I, the measurements of λ^{tr} at approximately 85 K are de-

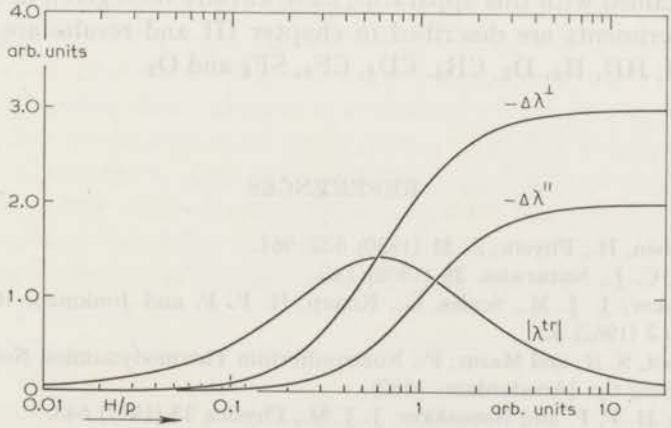

Fig. 2. Typical behaviour of $\Delta\lambda^{//}$, $\Delta\lambda^{\perp}$ and λ^{tr} as a function of H/p.

scribed, and results are given for N_2, CO, HD, O_2, NO, CH_4, CD_4 and CF_4. It is found that the experimental results can be described very well by the shape of the theoretical λ^{tr} curve as given in fig. 2. The magnitude of the effect, *i.e.*, the value of $|\lambda^{tr}/\lambda_0|_{max}$, is found to be of the order 10^{-3} for these gases. The experimental results are discussed in connection with theory.

In chapter II, results of λ^{tr} for H_2, D_2 and HD at temperatures between 20 K and 110 K are presented. These gases are particularly interesting at these temperatures, because only the lowest rotational levels are occupied, so that the effect of the rotational state on λ^{tr} can be seen here most prominently. Since the non-sphericity of the hydrogen isotopes is very small, inelastic collisions do occur very rarely. This gives rise to a somewhat simpler description of the Senftleben–Beenakker effect for these gases. The theory for the special case of the hydrogen isotopes, which has been developed recently[10]), allows a more detailed comparison between theory and experiments. A good agreement is found.

In chapter III, measurements on $\Delta\lambda^{//}$ and $\Delta\lambda^{\perp}$ are described. Before this research was initiated, results for these coefficients had already been reported by authors using hot wire type apparatus. This type of apparatus, which usually has a short response time and a relatively simple construction, has a few serious disadvantages. Firstly, Knudsen (or mean free path-) effects become of importance even at relatively high pressures. Furthermore, the temperature gradient has a $1/r$ pattern, so that $\nabla^2 T$ is non-zero throughout the apparatus. Therefore, a hot plate apparatus was developed, in which both difficulties are avoided. The essential feature of this apparatus is that it allows the determination of both $\Delta\lambda^{//}$ and $\Delta\lambda^{\perp}$ under the same experimental conditions by a rotation of the magnet over 90° around the apparatus. Thus one can determine quite accurately the ratio $\Delta\lambda^{\perp}/\Delta\lambda^{//}$ which is theoretically an interesting quantity, as it allows some general conclusions concerning the collision process of two rotating molecules[11]). Values of $\Delta\lambda^{\perp}/\Delta\lambda^{//}$ at saturation, obtained with this apparatus, have already been given in a letter[12]). These experiments are described in chapter III and results are presented for N_2, CO, HD, H_2, D_2, CH_4, CD_4, CF_4, SF_6 and O_2.

REFERENCES

1) Senftleben, H., Physik. Z. **31** (1930) 822, 961.
2) Gorter, C. J., Naturwiss. **26** (1938) 140.
3) Beenakker, J. J. M., Scoles, G., Knaap, H. F. P. and Jonkman, R. M., Phys. Letters **2** (1962) 5.
4) De Groot, S. R. and Mazur, P., Nonequilibrium Thermodynamics, North-Holland Publishing Cy. (Amsterdam, 1962).
5) Knaap, H. F. P. and Beenakker, J. J. M., Physica **33** (1967) 643.
6) Kagan, Yu. and Maksimov, L., Soviet Physics-JETP **24** (1967) 1272.

7) McCourt, F. R. and Snider, R. F., J. chem. Phys. **46** (1967) 2387.
8) Korving, J., Hulsman, H., Hermans, L. J. F., De Groot, J. J., Knaap, H. F. P. and Beenakker, J. J. M., J. Mol. Spectry. **20** (1966) 294.
9) Hermans, L. J. F., Fortuin, P. H., Knaap, H. F. P. and Beenakker, J. J. M., Phys. Letters **25A** (1967) 81.
10) Köhler, W. E. *et al.*, Z. Naturforsch., to be published.
11) Levi, A. C. and McCourt, F. R.,Physica **38** (1968) 415.
12) Hermans, L. J. F., Koks, J. M., Knaap, H. F. P. and Beenakker, J. J. M., Phys. Letters **30A** (1969) 139.

CHAPTER I

THE HEAT CONDUCTIVITY OF POLYATOMIC GASES IN MAGNETIC FIELDS

I. λ^{tr}

Synopsis

Transverse heat transport, *i.e.*, a heat flow perpendicular to both an applied temperature gradient and an externally applied magnetic field, has been measured for the gases N_2, CO, HD, O_2, NO, CH_4, CD_4 and CF_4 at approximately 85 K. Furthermore the signs of the rotational Landé g factors have been determined for these molecules.

1. *Introduction.* It is well known by now that the transport properties of polyatomic gases are changed by a magnetic field; indeed, for paramagnetic gases this was observed as early as 1930. During the last five years a great deal of experimental and theoretical work has been done on this subject, especially with respect to diamagnetic gases. For a survey see ref. 1. It has been found that even in gaseous systems both longitudinal and transverse effects occur[2–5]). For the thermal conductivity this corresponds to a heat transport perpendicular both to the applied temperature gradient and to the magnetic field. In metals such an effect called the Righi–Leduc effect[6,7]) after its discoverers, has been long known, but it was commonly thought (before 1966) that such an effect was necessarily restricted to a gas of charged particles. The existence of a transverse heat flow in polyatomic gases with rotational degrees of freedom was predicted independently by Knaap and Beenakker[8]), Kagan and Maksimov[9]) and McCourt and Snider[10]) around 1966. Their results were in accordance with the general irreversible thermodynamical treatment of these phenomena given earlier by de Groot and Mazur[11]). As a result, the simple Fourier law description of heat transport

$$\boldsymbol{q} = -\lambda_0 \boldsymbol{\nabla} T \tag{1}$$

has to be replaced (in the presence of an external field) by a more generalized Fourier law where the thermal conductivity λ_0 is replaced by a

second rank field-dependent tensor $\boldsymbol{\lambda}(\boldsymbol{H})$. This can be conveniently expressed in a matrix form as:

$$\begin{pmatrix} q_x \\ q_y \\ q_z \end{pmatrix} = - \begin{pmatrix} \lambda^{//}(H) & 0 & 0 \\ 0 & \lambda^{\perp}(H) & -\lambda^{\mathrm{tr}}(H) \\ 0 & \lambda^{\mathrm{tr}}(H) & \lambda^{\perp}(H) \end{pmatrix} \begin{pmatrix} \dfrac{\partial T}{\partial x} \\ \dfrac{\partial T}{\partial y} \\ \dfrac{\partial T}{\partial z} \end{pmatrix} \tag{2}$$

with the field directed along the x axis, *i.e.*, $\boldsymbol{H} = (H, 0, 0)$. The off-diagonal elements of the thermal-conductivity tensor determine the transverse heat flow, which may be compared with the Hall effect in electrical conductivity. The diagonal elements are analogous to magneto-resistance. In the field-free case, the matrix elements in eq. (2) become simply $\lambda^{//} = \lambda^{\perp} = \lambda_0$ and $\lambda^{\mathrm{tr}} = 0$, reducing to the trivial isotropic Fourier law. The field dependence of λ^{tr} is given by (see refs. 8–10):

$$\frac{\lambda^{\mathrm{tr}}}{\lambda_0} = -\psi \left\{ \frac{\Theta}{1+\Theta^2} + 2\frac{2\Theta}{1+4\Theta^2} \right\}; \qquad \Theta = C\,\frac{g\mu_N kT}{\hbar}\,\frac{H}{p}, \tag{3}$$

where the expression for Θ holds for diamagnetic gases, g is the rotational Landé g factor, μ_N is the nuclear magneton and p is the pressure. C and ψ are positive constants which depend on the molecular interactions in the gas. From this it is clear that Θ has the sign of g. Formally Θ can be written as $\Theta = \omega_p \tau$ where ω_p is the precession frequency of the rotational angular momentum around the field direction and τ is a characteristic time, which is (for this problem) of the order of the time between two collisions. In contrast to $\Delta\lambda^{//}$ $(= \lambda^{//} - \lambda_0)$ and $\Delta\lambda^{\perp}$ $(= \lambda^{\perp} - \lambda_0)$, which are even in Θ, λ^{tr} is odd in Θ and, since Θ is linear in H, the transverse heat flow changes sign when the field is reversed. As can be seen from eq. (3), Θ is also linear in g; thus measurements on λ^{tr} are very well suited for the determination of the sign of g.

An experimental verification of the existence of λ^{tr} (which was of a completely qualitative nature) was reported in a note on the sign of g[3]). Shortly after the appearance of this note somewhat more quantitative measurements were reported by Gorelik *et al.*[4]). The work of ref. 4 was, however, still rather qualitative, due to the great radiative heat losses at room temperature. The first quantitative measurements on N_2, CO, HD, O_2, NO, CH_4, CD_4 and CF_4[5]) were carried out at a lower temperature (85 K) where these radiative heat losses are greatly reduced. It is the purpose of this work to give full details of those measurements. Transverse heat transfer has also been observed in H_2 and D_2 but there, however, the situation is essentially different since:

a. the effect is about two orders of magnitude smaller,

b. these molecules are in very low rotational states, where the effect is strongly dependent on the rotational quantum numbers. This shows up both in a strong temperature dependence and in a different behaviour of the ortho and para modifications. For these reasons, the results for these gases at temperatures between 20 K and 110 K will be published in a separate article.

2. *Experimental.* 2*a*. Apparatus. A schematic diagram of the cylindrical apparatus is given in fig. 1. Under the influence of a magnetic field (x direction) a temperature gradient (z direction) causes a transverse heat flow (y direction). For this setup, eq. (2) gives:

$$q_y = -\lambda^{\perp} \frac{\partial T}{\partial y} + \lambda^{\mathrm{tr}} \frac{\partial T}{\partial z}. \tag{4}$$

Rather than measuring q_y directly, a corresponding temperature difference,

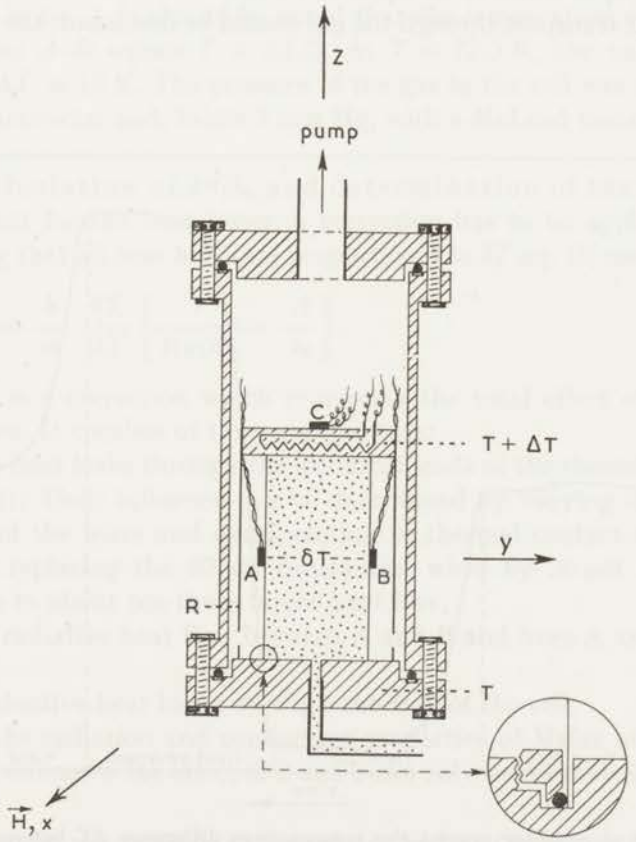

Fig. 1. Diagram of the apparatus.

δT, across the cell was measured because this is experimentally much simpler. In the stationary case in the absence of parasitic heat losses $q_y = 0$ and the observed temperature difference δT is found to be:

$$\frac{\delta T}{\Delta T} = \frac{w}{h} \frac{\lambda^{tr}}{\lambda_0} f\left(\frac{w}{h}\right), \tag{5}$$

where ΔT is the applied temperature difference, w is the width and h the height of the cell. In obtaining this result the difference between $\lambda^{\perp}$ and λ_0 has been neglected. The factor $f(w/h)$ accounts for the short-circuiting effect of the upper and lower plates and equals 1 when $h \gg w$. This factor is known from Hall experiments, where it has been studied extensively[12,13]). The results of these studies can be applied to the present measurements since the phenomenological equations governing the temperature pattern caused by transverse heat flow are similar to those governing the potential pattern in a Hall-sample. The fact that the present setup is cylindrical cannot be expected to cause serious deviations. For this system (with $w/h = \frac{1}{2}$) $f(w/h)$ is found to be equal to 0.93.

As the heat transport through the gas should be dominant, the cylindrical

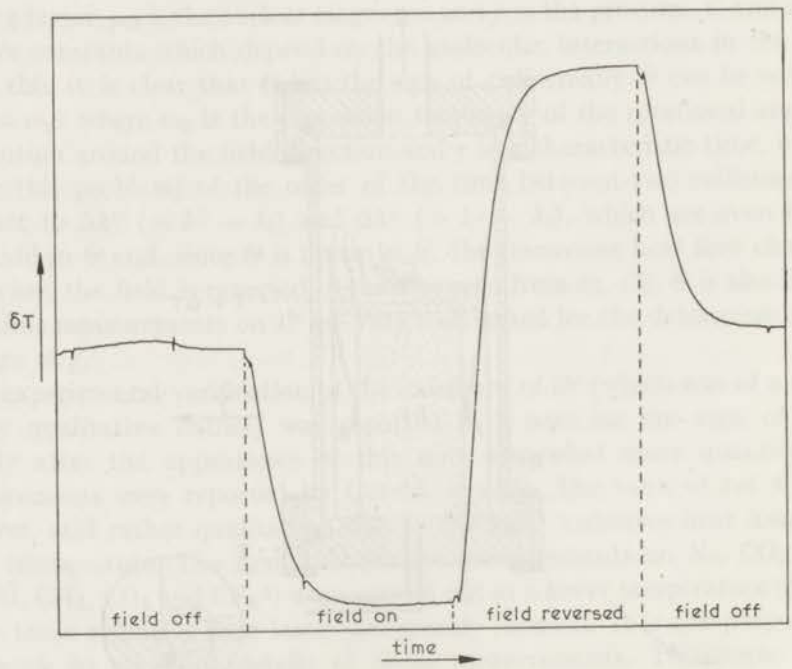

Fig. 2. A typical recorder graph: the temperature difference δT between A and B in the course of an experiment.

wall of the cell was constructed from a thin (0.19 mm) Mylar sheet† (which has a thermal conductivity coefficient five times smaller than that of glass) by melting two sides together with a hot wire. Vacuum-tightness was ensured by covering the seam with a thin layer of araldite (epoxy resin). The connections with the brass top and bottom of the cell were made with an indium "O"-ring construction as shown in a detail of fig. 1. The diameter of the cylinder is 23 mm, its height 45 mm. R is a radiation shield consisting of Mylar with a very thin aluminium coating to prevent radiative heat losses from the cell.

The temperature difference δT across the cell was measured by two thermistors A and B (Keystone Carbon Company, St. Marys, Pennsylvania, USA) with a temperature coefficient -3% K^{-1} at 85 K. The electrical connections were provided by 50 μm constantan wire. Thermistor C on the top plate provided the temperature $T + \Delta T$, while the temperature of the lower plate, which was in direct contact with the bath (liquid N_2 or O_2), was derived from the vapour pressure. A temperature resolution in δT up to 2×10^{-5} K could be achieved. A typical recorder plot of an experiment is shown in fig. 2. It should be noted that the temperature of the gas layer at the line A–B equals $T + \Delta T/2$. At $T = 77.3$ K, the value chosen for ΔT was $\Delta T \approx 15$ K. The pressure of the gas in the cell was measured with an oil manometer and, below 3 mm Hg, with a McLeod manometer.

2b. Calculation of λ^{tr}/λ_0 and determination of the heat losses. To account for the heat losses, a correction has to be applied to eq. (5). Assuming that all heat leaks are proportional to δT eq. (5) can be written as

$$\frac{\lambda^{tr}}{\lambda_0} = \frac{h}{w}\,\frac{\delta T}{\Delta T}\left\{\frac{1}{f(w/h)} + \frac{\Lambda}{\lambda_0}\right\}, \tag{6}$$

where Λ is a correction which represents the total effect of the parasitic heat losses. It consists of three components:

1. The heat leaks through the electrical leads of the thermistors A and B (see fig. 1): Their influence can be determined by varying the thermal resistance of the wires and extrapolating to thermal contact zero. This was done by replacing the 50 μm constantan wires by 30 μm copper, which gives rise to about ten times larger heat loss;

2. the radiative heat flow between A and B and from A and B outwards and;

3. conductive heat losses through the wall of the cell.

Since the radiation and conduction properties of Mylar at low temperatures are unknown the effect of 2 and 3 can only be estimated. This makes a

† We express our gratitude to Dupont de Nemours (Nederland) N.V. for helpful cooperation.

calculation of Λ rather inaccurate. On the other hand, it is also not possible to measure Λ directly in the evacuated cell – as is done in most heat conductivity experiments – because the temperature pattern of the wall, present when transverse heat transport occurs, cannot be easily reproduced. Therefore an indirect method was utilized for the measurement of Λ. This procedure entailed measuring δT after introducing a noble gas (which is not influenced by the field) into the vacuum jacket, keeping ΔT constant by increasing the heat input. Consequently, δT decreases to δT_n because of an increase of the heat losses due to the noble gas. Under the assumption that all heat losses occur parallel and that f and Λ are constants in this experimental setup, eq. (6) becomes:

$$\frac{\lambda^{tr}}{\lambda_0} = \frac{h}{w} \frac{\delta T_n}{\Delta T} \left\{ \frac{1}{f(w/h)} + \frac{\Lambda + g\lambda_n}{\lambda_0} \right\}, \tag{7}$$

where λ_n is the thermal conductivity of the noble gas, and g is a geometrical factor which does not complicate the procedure, since it will be shown to drop out of the final equation. From eqs. (6) and (7) the result

$$\frac{\delta T}{\delta T_n} = 1 + \frac{g}{1/f + \Lambda/\lambda_0} \frac{\lambda_n}{\lambda_0} \tag{8}$$

is immediately obtained. When λ_n is varied, *i.e.*, when different noble gases

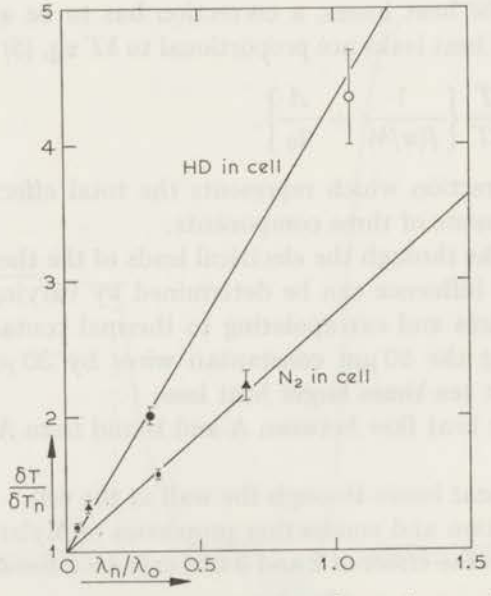

Fig. 3. Determination of the heat losses (see eq. (8)).
In measuring cell HD: In vacuum jacket ■ Kr; ▲ Ar; ● Ne; ○ He.
In measuring cell N_2: In vacuum jacket ■ Kr; ▲ Ar.

are introduced into the vacuum jacket, a plot of $\delta T/\delta T_n$ *vs.* λ_n/λ_0 should give a straight line according to eq. (8) with slope $g/(1/f + A/\lambda_0)$. Indeed, a straight line is found for HD in the measuring cell and the noble gases Kr, Ar, Ne and He in the vacuum jacket (see fig. 3). A similar result is obtained for an experiment with N_2 in the cell and Ar and Kr in the vacuum jacket. From the ratio of the slopes of the two lines (since g is eliminated) the value of A is obtained. This value checked to within 25% when compared with the one resulting from the aforementioned calculation. The value for A used in eq. (6) to calculate λ^{tr}/λ_0 is 8.8×10^{-5} watt cm^{-1} K^{-1}. The implication of this value is, that for gases like O_2, N_2 *etc.*, approximately half of the transverse heat flow is leaking away, while for HD the leakage is much less important (about 15%).

An error in A will affect all measured points for a given gas by the same factor so that a good comparison between experiment and theory for the field dependence of the effect is still possible. Estimating an uncertainty of about 20% in A, the error in $(\lambda^{tr}/\lambda_0)_{max}$ is found to be 3% for HD and about 10% for the other gases. For gases which have approximately equal thermal conductivity (CO, N_2, O_2, ...) the correction factor will be the same and hence it is possible to make there a meaningful comparison of the magnitudes of the effects.

3. *Experimental results and discussion.* The gases N_2, CO, HD, O_2, NO, CH_4 and CD_4 have been investigated at 85 K, while CF_4 was measured at 93 K because of its low vapour pressure. These gases had a purity of better than 99% except for CD_4 which contained 9% CHD_3 and 3% CO. The results of these measurements are given in figs. 4–6. In order to compare the experimental results with the functional behaviour described by the theoretical expression (3), the theoretical curve obtained from eq. (3) has been inserted in each plot by fitting the scale factors C and ψ to the maximum of the experimental curve. It can be seen that, with the exception of O_2, eq. (3) gives a good description of λ^{tr}/λ_0 as a function of H/p. A more refined theoretical expression for diamagnetic gases has been given by Levi and McCourt[14]) in which the effect of the next most important angular-momentum-dependent expansion term has been calculated; this results in eq. (3) being replaced by:

$$\frac{\lambda^{tr}}{\lambda_0} = -\psi\left\{\frac{\Theta}{1+\Theta^2} + 2\frac{2\Theta}{1+4\Theta^2}\right\} + \psi'\left\{\frac{\Theta'}{1+\Theta'^2}\right\}, \qquad (9)$$

where ψ' and Θ' are analogous to ψ and Θ of eq. (3). However, ψ' vanishes for gases having inverse collisions and will therefore be small for most gases. Only for strongly polar gases is ψ' expected to be important (see also ref. 1, page 305 and refs. 15 and 16). From the present measurements, a contribution of ψ' to λ^{tr} cannot be detected. If, however, Θ' is not too

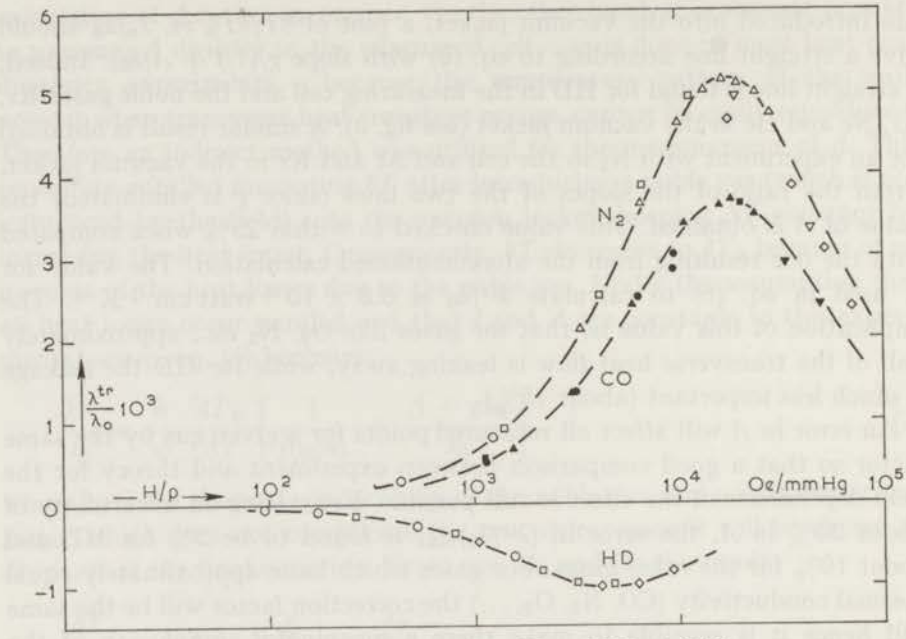

Fig. 4. λ^{tr}/λ_0 *vs.* H/p for N_2, CO and HD at 85 K.
N_2: ○ 7.2 mm Hg; □ 0.78 mm Hg; △ 0.30 mm Hg; ▽ 0.20 mm Hg; ◇ 0.125 mm Hg.
CO: ● 0.96 mm Hg; ■ 0.44 mm Hg; ▲ 0.36 mm Hg; ▼ 0.18 mm Hg.
HD: ○ 5.73 mm Hg; □ 1.89 mm Hg; △ 0.96 mm Hg.
---- theoretical curve (eq. (3)) scaled to the top of the experimental curve.

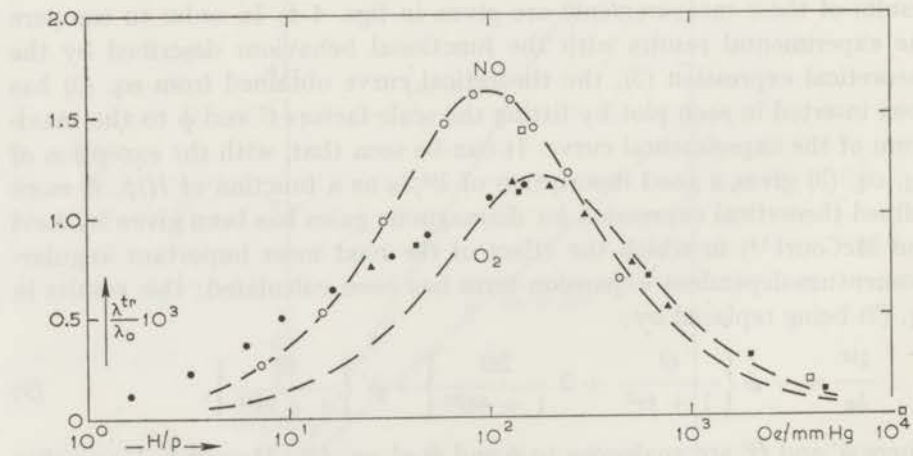

Fig. 5. λ^{tr}/λ_0 *vs.* H/p for NO and O_2 at 85 K. NO was measured in a liquid air bath ($T \approx 80$ K; $\Delta T = 10$ K) because of its low vapour pressure at 77 K.
NO: ○ 0.20 mm Hg; □ 0.26 mm Hg.
O_2: ● 2.7 mm Hg; ■ 0.8 mm Hg; ▲ 0.5 mm Hg.
--- theoretical curve (eq. (3)) scaled to the top of the experimental curve.

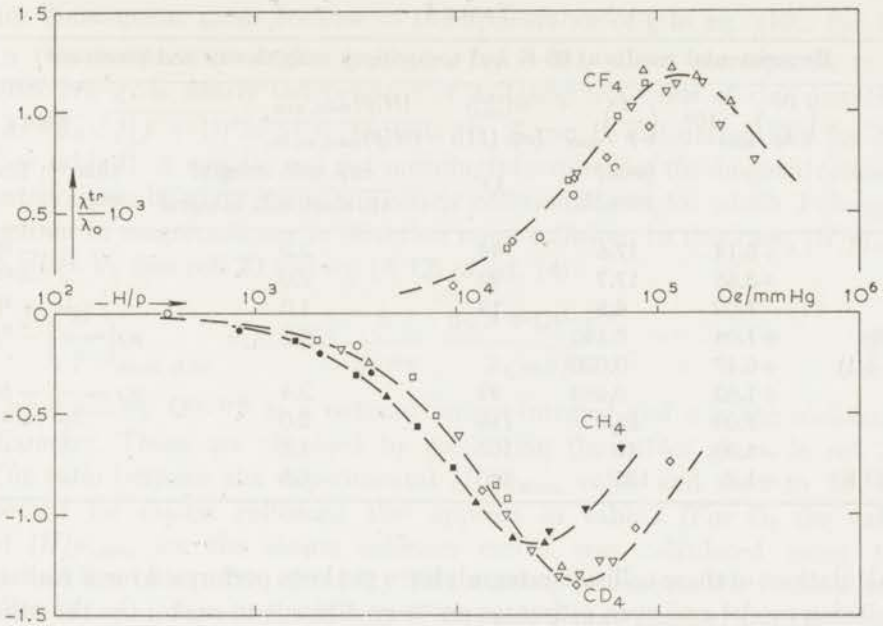

Fig. 6. λ^{tr}/λ_0 *vs.* H/p for CH_4 and CD_4 at 85 K and for CF_4 at 93 K. CF_4 was measured in a liquid O_2 bath ($T = 90$ K, $\Delta T = 6$ K) because of its low vapour pressure at 77 K.
CH_4: ● 2.4 mm Hg; ■ 0.94 mm Hg; ▲ 0.32 mm Hg; ▼ 0.14 mm Hg.
CD_4: ○ 2.8 mm Hg; □ 0.5 mm Hg; △ 0.3 mm Hg; ▽ 0.2 mm Hg; ◇ 0.08 mm Hg.
CF_4: ○ 0.15 mm Hg; □ 0.11 mm Hg; ◇ 0.10 mm Hg; △ 0.05 mm Hg; ▽ 0.04 mm Hg.
---- theoretical curve (eq. (3)) scaled to the top of the experimental curve.

different from Θ, a possible small contribution of ψ' is easily masked, and cannot be excluded, since both terms have a very similar functional behaviour on Θ and Θ'. In conclusion it can be said that eq. (3) gives a good description of this phenomenon.

Table I shows the experimental data characterizing the curves. As discussed earlier, no accurate results for λ^{tr}/λ_0 have been obtained at room temperature. Therefore only a qualitative comparison can be made between the values of $(\lambda^{tr}/\lambda_0)_{max}$ given here and results obtained for $\Delta\lambda^{\perp}/\lambda_0$ and $\Delta\lambda^{//}/\lambda_0$ at room temperature[17,18]). It is found that these quantities have, for all gases, the same order of magnitude as $(\lambda^{tr}/\lambda_0)_{max}$. A more useful comparison can be made only in connection with the results of the low temperature measurements of $\Delta\lambda^{\perp}/\lambda_0$ and $\Delta\lambda^{//}/\lambda_0$, which are still in progress[19]).

A detailed theoretical interpretation of the magnitude of $(\lambda^{tr}/\lambda_0)_{max}$ is rather complicated since it is directly determined by off-diagonal collision integrals which are themselves directly connected to the non-spherical part of the intermolecular interaction (see eq. (30) of ref. 14). No

TABLE I

Experimental results at 85 K and comparison with theory and literature

	$\left(\frac{\lambda^{tr}}{\lambda_0}\right)_{max} 10^3$	$\left(\frac{H}{p}\right)_{max}$ (kOe/mm Hg)	$\mathfrak{S}^{(1200)}_{(1200)}$ (eq. (11)) Å^2	$\frac{(H/p)_{max,\,exp}}{(H/p)_{max,\,el.\,th.}} = \frac{\text{exp. coll. integral}}{\text{th. elast. coll. integral}}$	Sign g this exp.	Sign g literature
N_2	+5.14	17.6	94	2.2	−	−[2)3)31)]
CO	+3.66	17.7	92	2.0	−	−[22)23)31)]
HD	−1.02	4.5	19	1.0	+	+[2)3)32)33)]
O_2 ($\sigma = 0$)	+1.04	0.190		4.3	$\mu_J \sim$ −	−[8)31)]
($\sigma = \pm 1$)	+0.47	0.020				
NO	+1.62	0.098	99	2.4	$\mu_J \sim$ −	−[31)]
CH_4	−1.08	25.0	110	2.0	+	+[31)34)]
CD_4	−1.30	40	100	1.8	+	
CF_4 (at 93 K)	+1.2	125	140	1.5	−	

calculations of these collision integrals have yet been performed for a realistic collision model and even estimates are very difficult to make. On the other hand, a fairly realistic estimate can be made for the diagonal collision integral determining the position of the maximum, *i.e.*, $(H/p)_{max}$, of the λ^{tr}/λ_0 curve. From eq. (3), the maximum of the curve is seen to occur for $\Theta_{max} = 0.6153$ and, using this value, an expression for $(H/p)_{max}$ can be derived from eq. (A.11) of ref. 14: this expression is:

$$\left(\frac{H}{p}\right)_{max} = 0.6153\,\frac{\hbar}{|g|\,\mu_N k T}\,\frac{\langle [J]^{(2)}_{ij}\, W_k \Re_0 W_k [J]^{(2)}_{ji}\rangle}{\frac{1}{4}\langle 4J^4 - 3J^2\rangle}, \tag{10}$$

where $\langle\ \rangle$ denotes an average using the equilibrium distribution function (divided by n) and summing over equal indices, while $\Re_0 = -\mathscr{J}_0/n$ where n is the number density and $\mathscr{J}_0$ is the (dissipative) collision operator as defined in eq. (4) of ref. 14. Both averages in eq. (10) are density independent and positive†. From the observed values of $(H/p)_{max}$ we can now calculate the quantity

$$\mathfrak{S}^{(1200)}_{(1200)} = \frac{\langle [J]^{(2)}_{ij}\, W_k \Re_0 W_k [J]^{(2)}_{ji}\rangle}{\frac{1}{4}\langle 4J^4 - 3J^2\rangle}\,\frac{1}{\langle v_{rel}\rangle}. \tag{11}$$

We have divided by $\langle v_{rel}\rangle = \sqrt{8kT/\pi\mu}$ where μ is the reduced mass $\mu = \frac{1}{2}$ m, so that $\mathfrak{S}$ has the dimension of a cross section. The values for $\mathfrak{S}$ obtained in this way are given in table I. Though such a procedure is only meaningful

† The square bracket integral h^{44}_{sph} used in ref. 14 is related to the above expression by

$$h^{44}_{sph} = \tfrac{1}{15} n^2 \left(\frac{20}{\langle 4J^4 - 3J^2\rangle}\right)^2 \langle [J]^{(2)}_{ij} W_k\, \Re_0\, W_k [J]^{(2)}_{ji}\rangle.$$

for diamagnetic gases because of the appearance of g in eq. (10), for NO in this temperature region $|\mu_J|/(\mu_N\sqrt{J(J+1)})$, which corresponds to an effective g, is nearly independent of J. Using the value of this quantity, $|\mu_J|/(\mu_N\sqrt{J(J+1)}) = 51$ in formula 10, $\mathfrak{S}$ can be calculated also for NO (see table I). A simple, and yet meaningful estimate of the diagonal collision integral can be given using the elastic collision model for which $\boldsymbol{J}$ changes neither in magnitude nor in direction upon collision. In this case, $(H/p)_{max}$ is given by (see ref. 20 and eq. (A.12) of ref. 14):

$$\left(\frac{H}{p}\right)_{\text{max, el.th.}} = 0.6153\,\frac{\hbar}{|g|\,\mu_N}\,\frac{8\sqrt{\pi}\,\sigma^2\Omega^{(1,1)\star}}{3\sqrt{mkT}}. \tag{12}$$

The quantity $\Omega^{(1,1)\star}$ is a reduced omega-integral and σ is the molecular diameter. These are obtained by consulting the tables given in ref. 21. The ratio between the experimental $(H/p)_{max}$ value and that to be expected for elastic collisions also appears in table I (For O_2 the value of $(H/p)_{max}$ for the elastic collision model was calculated using the second line of eq. (52) of ref. 8.) This number represents the realistic collision integral, for which not only $\boldsymbol{W}$ but also $\boldsymbol{J}$ may change, and the (theoretical) elastic collision integral. Indeed, for a gas such as HD for which inelastic collisions are relatively infrequent, a ratio of almost 1 is found. The other tabulated gases, where inelastic collisions occur frequently, show that the inelasticity increases the cross section by a factor of approximately 2. A similar analysis of the even in $\boldsymbol{H}$ thermal conductivity measurements at room temperature[18,19]) shows the same behaviour.

As discussed in the introduction this experiment yields also the sign of the rotational g factor for non-paramagnetic molecules. The observed sign of g is also listed in table I. In all cases where comparison is possible there is agreement with literature. The sign of g for CO confirms the conjecture of Rosenblum *et al.*[22]) in their determination of the sign of the electric dipole in CO as C^-O^+ (see also ref. 23).

The special cases of the paramagnetic molecules O_2 and NO can now be briefly discussed. In the case of oxygen the exceptional behaviour is basically due to the possession by O_2 of a resultant electronic spin which gives rise to a $^3\Sigma$ ground electronic state. Hence, the spin angular momentum $\boldsymbol{S}$ ($S = 1$) can have three orientations with respect to the total angular momentum $\boldsymbol{J}$ with components $\sigma = +1$, -1 or 0 along $\boldsymbol{J}$. Accordingly, the magnetic moments along $\boldsymbol{J}$ are, respectively (see *e.g.* ref. 8):

$$\begin{aligned} \boldsymbol{\mu} &\approx -2\mu_B\boldsymbol{J}/J \qquad (\sigma = +1),\\ \boldsymbol{\mu} &\approx +2\mu_B\boldsymbol{J}/J \qquad (\sigma = -1),\\ \boldsymbol{\mu} &\approx -2\mu_B\boldsymbol{J}/J^2 \qquad (\sigma = 0). \end{aligned} \tag{13}$$

Multiplet Σ states, being nearly degenerate, are easily mixed via the mecha-

nism of molecular collisions and hence great care must be taken when expressions for these field effects are desired. From spectroscopic work on the energy level structure of the O_2 molecule[24]), it is known that in the absence of an external magnetic field the $\sigma = 0$ state is separated from the $\sigma = \pm 1$ states by approximately 60 GHz while the separation between the $\sigma = +1$ and the $\sigma = -1$ states varies between 1 and 4 GHz depending on the rotational state of the molecule. In the experiments described here, the inverse of the time of free flight (commonly called the collision frequency) was of the order of 0.01 GHz. Thus in a certain sense, the three σ states can be treated as well separated, each state corresponding to the molecule having the magnetic moment as given by eq. (13). This is still the case in low external magnetic fields, where the Zeeman levels of the different σ states do not yet overlap. As a first consequence it can be expected that under the present experimental conditions O_2 follows an H/p law as is indeed found (see fig. 5). This behaviour is in contrast to that found for viscosity measurements[25, 26]) which were performed under different conditions (high pressures and high fields).

Since it is the triplet structure of the ground state of O_2 which underlies all observations depending in any way on the angular momenta of the O_2 molecule, it will be safe to correlate, in some average sense, the observed properties with the magnetic moments associated with these states (see eq. (13)). For this reason certain of the features such as two humps in the longitudinal thermal conductivity components $\Delta\lambda^{//}/\lambda_0$ and $\Delta\lambda^{\perp}/\lambda_0$, the relative positions of the $(H/p)_{\frac{1}{2}}$ values of the humps, and the existence of a transverse effect (although having only a single peak at an H/p value corresponding to the $\sigma = 0$ state) could be obtained[8]) using the comparatively crude model introduced by Kagan and Maksimov[20]), where the σ states do not change upon collision. In a second paper[9]) Kagan and Maksimov pointed out that if this simplification is dropped the contributions to the transverse effect of the $\sigma = +1$ and $\sigma = -1$ states no longer cancel, thus giving rise to a second peak at an appreciably lower H/p value, as was confirmed in the work of Gorelik *et al.*[4]) at room temperature.

The present data behave as is to be expected along these lines of thought:

a) The λ^{tr}/λ_0 curve for O_2 cannot be described with the simple theoretical expression given in eq. (3).

b) The experimental curve may be decomposed into two contributions of the form of eq. (3) (see fig. 7). The maxima of the two contributions occur at 20 Oe/mm Hg and 190 Oe/mm Hg. The ratio of the positions of these maxima has the value 9.5 in good agreement with the value 8.5 predicted by the simple treatment in which the σ states cannot be mixed via molecular collisions. Since this ratio varies as $\sqrt{T}$ this is also in agreement with the results of Gorelik *et al.*[4]) who found a value 16 for this ratio at room temperature.

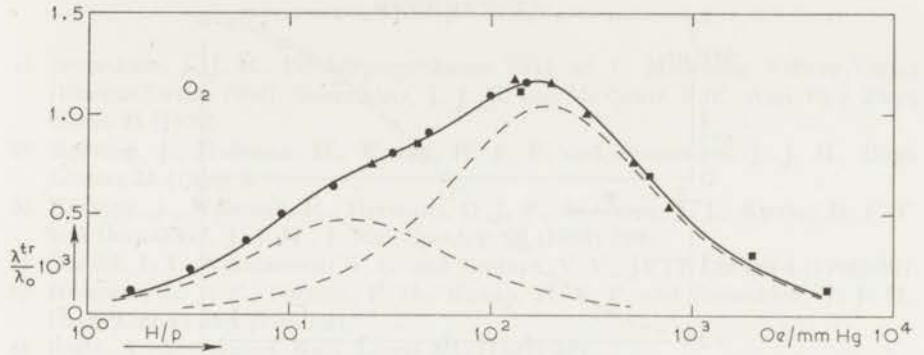

Fig. 7. An analysis of the results for O_2.
——— Superposition of two curves of the shape of eq. (3) at 20 Oe/mm Hg ($\lambda^{tr}/\lambda_0 = 0.47 \times 10^{-3}$) and 190 Oe/mm Hg ($\lambda^{tr}/\lambda_0 = 1.04 \times 10^{-3}$).
● ■ ▲ Experimental points taken from fig. 5.

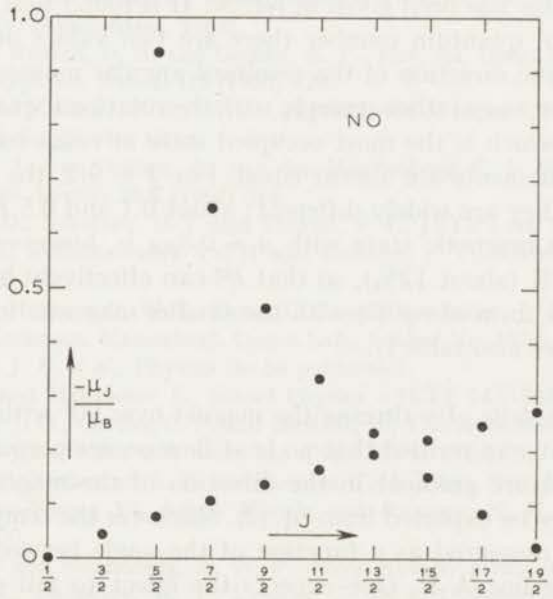

Fig. 8. The magnetic moment along the axis of rotation in Bohr magnetons as a function of the rotational quantum number J for NO (see refs. 29 and 30). Due to intermediate L–S coupling the spin is gradually decoupled from the rotational axis by an increasing amount of rotation of the nuclei.

For a complete analysis of these phenomena the full internal Hamiltonian of the O_2 molecule has to be taken into account[27,28]).

It is found that λ^{tr} for NO can be described as a unique function of the form given by eq. (3), although NO is a $^2\Pi$ state. The $^2\Pi$ states for NO have been treated explicitly by Hill[29]); a more convenient expression for

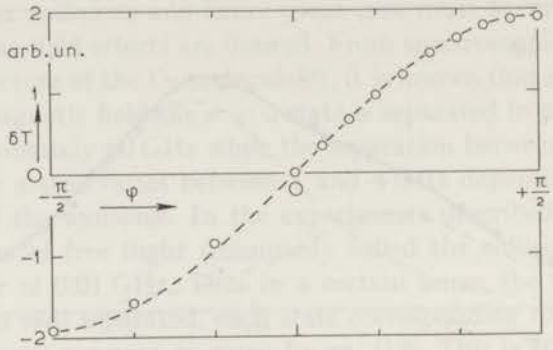

Fig. 9. Observed temperature difference between A and B as a function of the angle between the magnetic field and the line A–B for N_2 at $(H/p)_{max}$.
---- theoretical curve scaled at $\varphi = \pi/2$.

the Landé g factor has been given in ref. 30. It is found that for each value of the rotational quantum number there are two values of the magnetic moment along the direction of the resultant angular momentum, $\boldsymbol{J}$. These values, moreover, vary rather strongly with the rotational quantum number. For $J = 15/2$, which is the most occupied state at room temperature, the two magnetic moments are almost equal. For $J = 9/2$, the most occupied state at 85 K, they are widely different: about 0.1 and 0.5 Bohr magneton (see fig. 8). The magnetic state with $\mu \approx 0.5\mu_B$ is, however, only slightly occupied at 85 K (about 12%), so that λ^{tr} can effectively be described by one curve of the form of eq. (3) with the smaller magnetic moment. This is indeed found (see also table I).

4. *Consistency tests.* By turning the magnet over 90° with respect to the measuring cell it was verified that no heat flow occurs perpendicular to the applied temperature gradient in the direction of the magnetic field. This should obviously be expected from eq. (2). Moreover the temperature difference A–B was measured as a function of the angle between the field direction and the line A–B. One expects the effect to fall off as $\delta T(\varphi) = \delta T(\pi/2) \sin \varphi$. This is indeed found as illustrated in fig. 9.

Experiments were also performed with the noble gases Ar and He in the measuring cell. As should be expected there, no transverse heat flow could be detected.

REFERENCES

1) Beenakker, J. J. M., Festkörperprobleme VIII, ed. O. Madelung, Vieweg Verlag (Braunschweig, 1968); Beenakker, J. J. M. and Mc Court, F. R., Ann. Rev. Phys. Chem. **21** (1970).
2) Korving, J., Hulsman, H., Knaap, H. F. P. and Beenakker, J. J. M., Phys. Letters **21** (1966) 5.
3) Korving, J., Hulsman, H., Hermans, L. J. F., de Groot, J. J., Knaap, H. F. P. and Beenakker, J. J. M., J. Mol. Spectry. **20** (1966) 294.
4) Gorelik, L. L. ,Nikolaevskii, V. G. and Sinitsyn, V. V., JETP Letters **4** (1966) 307.
5) Hermans, L. J. F., Fortuin, P. H., Knaap, H. F. P. and Beenakker, J. J. M., Phys. Letters **25A** (1967) 81.
6) Righi, A., Atti Accad. Nazl. Lincei **3**(1) (1887) 481.
7) Leduc, A., J. Physics **6** (1887) 373.
8) Knaap, H. F. P. and Beenakker, J. J. M., Physica **33** (1967) 643 (Commun. Kamerlingh Onnes Lab., Leiden, Suppl. No. 124*a*).
9) Kagan, Yu. and Maksimov, L., Soviet Physics – JETP **24** (1967) 1272.
10) McCourt, F. R. and Snider, R. F., J. chem. Phys. **46** (1967) 2387.
11) de Groot, S. R. and Mazur, P., Nonequilibrium Thermodynamics, North-Holland Publishing Cy. (Amsterdam, 1962).
12) Isenberg, I., Russell, B. R. and Greene, R. F., Rev. sci. Instr. **19** (1948) 685.
13) Frank, V., Appl. sci. Res. B III (1953) 129.
14) Levi, A. C. and McCourt, F. R., Physica **38** (1968) 415 (Commun. Kamerlingh Onnes Lab., Leiden, Suppl. No. 126*a*).
15) de Groot, J. J., van Oosten, A., van den Meydenberg, C. J. N. and Beenakker, J. J. M., Phys. Letters **25A** (1967) 348.
16) Borman, V. D., Nikolaev, B. I. and Troyan, V. I., JETP Lett. **9** (1969) 134.
17) Gorelik, L. L., Redkoborodyi, Yu. N. and Sinitsyn, V. V., Soviet Physics – JETP **21** (1965) 503.
18) Korving, J., Honeywell, W. I., Bose, T. K. andBeenakker, J. J. M., Physica **36** (1967) 198 (Commun. Kamerlingh Onnes Lab., Leiden No. 357*c*).
19) Hermans, L. J. F. *et al.*, Physica (to be published).
20) Kagan, Yu. and Maksimov, L., Soviet Physics – JETP **14** (1962) 604.
21) Hirschfelder, J. O., Curtiss, C. F. and Bird, R. B., The Molecular Theory of Gases and Liquids, John Wiley and Sons, Inc. (New York, 1954).
22) Rosenblum, B, Nethercot, A. H. and Townes, C. H., Phys. Rev. **109** (1958) 400.
23) Ozier, I., Pon-Nyong Yi, Ashok Khosla and Ramsey, N. F., J. chem. Phys. **46** (1967) 1530.
24) Tinkham, M. and Strandberg, M. W. P., Phys. Rev. **97** (1955) 937, 951.
25) Kikoin, I. K., Balashov, K. I., Lasarev, S. D. and Neushtadt, P. E., Phys. Letters **24A** (1967) 165.
26) Hulsman, H., private communication.
27) Coope, J. A. R., McCourt, F. R. and Snider, R. F., J. chem Phys., to be published.
28) Coope, J. A. R., Moraal, H. and Snider, R. F., J. chem. Phys. to be published.
29) Hill, E. L., Phys. Rev. **34** (1929) 1507.
30) Dousmanis, G. C., Sanders, T. M. and Townes, C. H., Phys. Rev. **100** (1955) 1735.
31) Scott, G. G., Sturner, H. W. and Williamson, R. M., Phys. Rev. **158** (1967) 117.
32) Herzberg, G., Spectra of Diatomic Molecules, D. van Nostrand Cy., Inc. (Princeton, New Jersey, 1961).
33) Scott, G. G., Sturner, H. W. and Williamson, R. M., Phys. Letters **25A** (1967) 573.
34) Anderson, C. H. and Ramsey, N. F., Phys. Rev. **149** (1966) 14.

CHAPTER II

THE HEAT CONDUCTIVITY OF POLYATOMIC GASES IN MAGNETIC FIELDS

II. λ^{tr} AS A FUNCTION OF TEMPERATURE FOR THE H_2-ISOTOPES

Synopsis

For gaseous hydrogen isotopes at temperatures between 22 K and 110 K, measurements are reported on transverse heat flow, which occurs under the influence of a magnetic field. For HD, the effect is found to be much larger than for H_2 and D_2. The observed strong temperature dependence of the effect is compared with theoretical expressions. Mixtures of para hydrogen with ortho hydrogen as well as mixtures of ortho deuterium with helium have also been investigated.

1. *Introduction.* In the previous chapter[1]) results were published on transverse heat flow – *i.e.*, heat flow perpendicular to both applied temperature gradient and magnetic field – for several polyatomic gases at approximately 85 K. It was found that for the gases studied the maximum of the effect, *i.e.*, $|\lambda^{tr}/\lambda_0|_{max}$ is of the order 10^{-3}, this magnitude being determined by the non-spherical part of the intermolecular interaction. For HD an effect of 1×10^{-3} was found. This molecule has a strong loaded sphere character: rotation around an off-center axis gives rise to a relatively large apparent non-sphericity. For the homonuclear hydrogen isotopes the situation is quite different. First, the non-spherical part of the interaction potential is much smaller, as is known from other experiments[2]). Consequently, the value of $|\lambda^{tr}/\lambda_0|_{max}$ can be expected to be much smaller for these molecules. Secondly, H_2 and D_2 appear in two modifications depending on the total nuclear spin of the molecule, one having even rotational states only (para H_2 and ortho D_2), the other having odd rotational states (ortho H_2 and para D_2). Since H_2 and D_2 are in low rotational states due to their small moments of inertia, the dependence of λ^{tr} on the rotational quantum number j can be studied by varying the temperature and by investigating the ortho and para modifications, which makes these gases particularly interesting.

In the course of the experiments close contact has existed between experimentalists and theoreticians working in this field. This cooperation has led to a simultaneous development of experiment and theory. As a consequence, the experimental data for the hydrogen isotopes can now be compared with calculations as performed by Köhler *et al.*[3]).

2. *Experimental method.* The apparatus used is the one described in chapter I. A temperature difference is applied between two parallel plates, of which the top one is at a temperature of $T_0 + \Delta T$ and the bottom one at T_0. The transverse heat flow is measured halfway between the two plates. Using $T_0 = 20.4$ K or $T_0 = 77.3$ K, the temperature ranges from 22 to 26 and from 85 to 110 K could be covered by varying the applied temperature difference ΔT. The thermistors used in the whole temperature range were of the type Keystone L 0904–125 K-H-T_2. Since the effects which were measured are two or three orders of magnitude smaller than those for gases like N_2 and O_2, great care had to be taken with respect to the purity of the gases. It was verified that the amount of nonisotopic impurities did not exceed 0.01%. The D_2 which was used contained about 1% of HD. As a result, the measured values of $|\lambda^{tr}/\lambda_0|_{max}$ may be too high by approximately 10% for normal D_2, and by about 3% for ortho D_2 (see table I).

TABLE I

Experimental results and comparison with theory

	T	$-10^6\left(\frac{\lambda^{tr}}{\lambda_0}\right)_{max}$	$\left(\frac{H}{p}\right)$	$\Im_{(1200)}^{(1200)}$ (eq. (4))	$\frac{(H/p)_{max,exp}}{(H/p)_{max,el.th.}} = \frac{\text{exp. coll. integral}}{\text{th. elast. coll. integral}}$
	K		kOe/torr	Å²	
HD	21.9	29	(14)		
	23.6	52	(14)		
	26.2	84	11	25	0.9
	85	1020	4.5	19	1.0
para H_2	86	31	(3)		
	100	52	(3)		
	110	68	3.0	15	0.9
normal H_2	26.4	< 2	—		
(75% ortho, 25% para)	85	< 3	—		
	100	< 3	—		
	110	3	(3.5)		
ortho D_2	85	310	6.2	20	1.1
normal D_2	26.4	7	(16)		
(67% ortho, 33% para)	85	114	5.8	18	1.0

3. *Experimental results and discussion.* Measurements were performed (see table I) on HD, para H_2, normal H_2 ($\frac{3}{4}$ ortho, $\frac{1}{4}$ para), ortho D_2 and normal D_2 ($\frac{2}{3}$ ortho, $\frac{1}{3}$ para). Furthermore, pH$_2$–oH$_2$ mixtures and oD$_2$–He mixtures were investigated.

The theoretical expression for λ^{tr} as given in ref. 4 for diamagnetic gases can be written in the form

$$\frac{\lambda^{tr}}{\lambda_0} = -\psi_{12}\left\{\frac{\xi_{12}}{1+\xi_{12}^2} + 2\,\frac{2\xi_{12}}{1+4\xi_{12}^2}\right\} + \psi_{11}\left\{\frac{\xi_{11}}{1+\xi_{11}^2}\right\}, \tag{1}$$

with

$$\xi_{ij} = C_{ij}\,\frac{g\mu_N kT}{\hbar}\,\frac{H}{p}. \tag{2}$$

Here $\lambda^{tr} = \lambda_{zy}$, g is the rotational g factor, μ_N is the nuclear magneton, p is the pressure and H is the magnetic field. The positive coefficients ψ_{12} and C_{12} † depend through collision integrals on the molecular interaction potential, and they correspond to the contribution of the $\boldsymbol{W}[\boldsymbol{J}]^{(2)}$ anisotropic term which occurs in the expansion of the distribution function in terms of

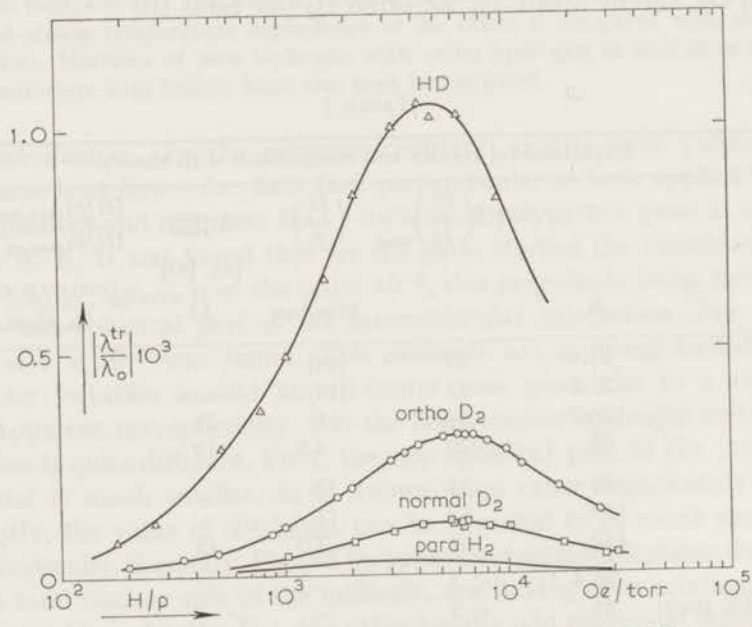

Fig. 1. $|\lambda^{tr}/\lambda_0|$ *vs.* H/p for HD, ortho D_2 and normal D_2 at 85 K, and for para H_2 (see also fig. 5) at 86 K. For normal H_2 it was found that $|\lambda^{tr}/\lambda_0|_{max} < 3 \times 10^{-6}$.

† In comparing the expressions given here with those of ref. 4 it should be noted that the quantity in ref. 4 which corresponds to C_{12} used here is negative, whereas the quantity which corresponds to C_{11} is positive.

velocity, $\boldsymbol{W}$, and angular momentum, $\boldsymbol{J}$. Similarly, the positive coefficients ψ_{11} and C_{11} correspond to the contribution arising from the $\boldsymbol{WJ}$ term. However, as follows from the results obtained in chapter III, the contribution from this term is, for non-polar gases, at the most 5%, but usually much less. Consequently, ψ_{11} can be neglected for the hydrogen isotopes when describing λ^{tr} using eq. (1). In fig. 1, where the results of the measurements at 85 and 86 K are presented, theoretical curves according eq. (1) with $\psi_{11} = 0$ have been drawn through the experimental points, adapting ψ_{12} and C_{12} to the experiment. These curves describe the experimental points very well. The magnitude of the effect, *i.e.*, the value of ψ_{12}, differs greatly for the gases investigated in this research.

3*a*. *HD*. As stated in the introduction, due to its loaded sphere character HD has a much larger effective non-sphericity than H_2 and D_2. Since ψ_{12} is strongly related to the non-spherical part of the interaction potential, the dominant part of which is in this case of the $P_1(\cos\chi)$ type, the effect for HD at 85 K is large in spite of the fact that more than half of the molecules are not rotating at this temperature (see fig. 2). These molecules are not influenced by the field since they lack a magnetic moment coupled to the molecular axis, and therefore do not contribute to λ^{tr}. To find the relation between ψ_{12} and the fraction of rotating molecules, measurements were performed at 21.9 K, 23.6 K and 26.2 K, where the fraction of rotating ($j = 1$) molecules varies strongly with temperature. As can be seen from fig. 3, $|\lambda^{tr}/\lambda_0|_{max}$ or ψ_{12} is proportional to $x_{j=1}$. It is remarked that the result obtained at 85 K, where $x_{j\neq 0} = 0.42$, also fits this proportionality within a factor 1.5. This linear behaviour of HD is quite similar

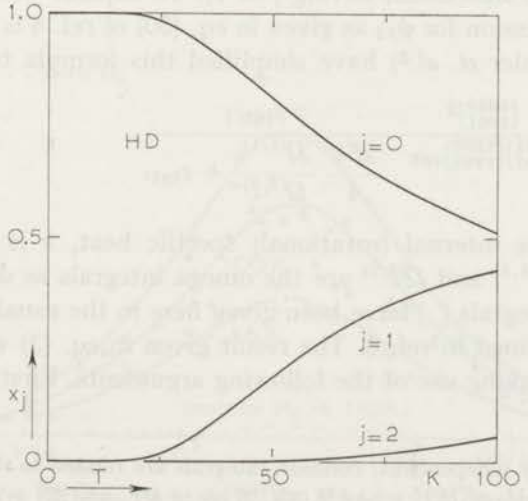

Fig. 2. The occupation of the rotational levels for HD as a function of temperature.

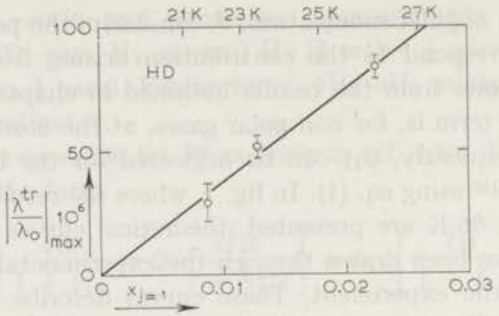

Fig. 3. The measured values of $|\lambda^{tr}/\lambda_0|_{max}$ for HD *vs.* fraction of rotating molecules.

to the behaviour of mixtures of polyatomic gases with (non-rotating) noble gases of approximately the same mass, as found both in the older experiments on O_2 [5]) and in recent experiments on HD [6]). The linear dependence on $x_{j=1}$ can be understood qualitatively if one assumes that the effect is determined by the coupling of the $\boldsymbol{W}[\boldsymbol{J}]^{(2)}$ term with the translational heat flux, and that the coupling of $\boldsymbol{W}[\boldsymbol{J}]^{(2)}$ to the internal heat transport is much less important [3]).

3*b*. *H_2 and D_2*. Since these molecules have a very small non-sphericity, the effect is a few orders of magnitude smaller than for O_2 and N_2, and considerably smaller than the effect for the loaded-sphere molecule HD (see fig. 1 and table I). For H_2 it is found that for the para modification $|\lambda^{tr}/\lambda_0|_{max}$ is, at 85 K, of the order 10^{-5}, while for normal H_2 no effect could be detected. This may seem rather surprising, since at 85 K only 1% of the para molecules rotate ($j = 2$), while in normal H_2 75% of the molecules rotate (the ortho molecules, having $j = 1$). To explain this behaviour, the theoretical expression for ψ_{12} as given in eq. (30) of ref. 4 is considered. For H_2 and D_2, Köhler *et. al.*[3]) have simplified this formula to:

$$\psi_{12} = \tfrac{1}{2} \frac{\left[\begin{smallmatrix}1200\\1001\end{smallmatrix}\right]^2}{\left[\begin{smallmatrix}1001\\1001\end{smallmatrix}\right]\left[\begin{smallmatrix}1200\\1200\end{smallmatrix}\right]_{sph}} \frac{c_{int}}{\frac{25k}{4}\frac{\Omega^{(1,1)}}{\Omega^{(2,2)}} + c_{int}}, \tag{3}$$

where c_{int} is the internal (rotational) specific heat, k is the Boltzmann constant and $\Omega^{(1,1)}$ and $\Omega^{(2,2)}$ are the omega integrals as defined in ref. 7. The collision integrals [ ] have been given here in the usual square-bracket notation* as defined in ref. 8. The result given in eq. (3) was obtained by Köhler *et al.*, making use of the following arguments. First, for H_2 and D_2

* These (density independent) collision integrals are related to those used in ref. 4 by: $n^2\left[\begin{smallmatrix}1010\\1001\end{smallmatrix}\right] = +h^{12}$, $n^2\left[\begin{smallmatrix}1001\\1001\end{smallmatrix}\right] = +h^{22}$, $n^2\left[\begin{smallmatrix}1200\\1010\end{smallmatrix}\right] = +h^{14}$, $n^2\left[\begin{smallmatrix}1200\\1001\end{smallmatrix}\right] = +h^{24}$ and $n^2\left[\begin{smallmatrix}1200\\1200\end{smallmatrix}\right]_{sph} = +h^{44}_{sph}$.

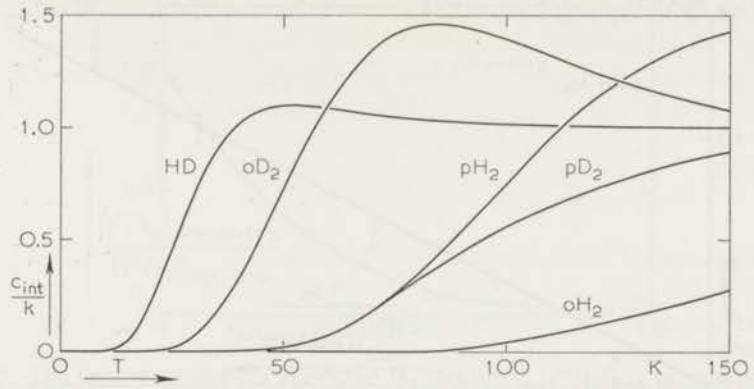

Fig. 4. Internal (rotational) specific heat *vs.* temperature for HD, ortho D_2, para D_2, para H_2 and ortho H_2.

there is slow exchange between translational and rotational energy transport, because only 1 in approximately 1000 collisions are energetically inelastic[2]). Secondly, it follows from theoretical considerations[3,9]) that in the absence of inelastic collisions the coupling between $\boldsymbol{W}[\boldsymbol{J}]^{(2)}$ and the rotational energy transport is dominant, so that the collision integral $[^{1200}_{1001}]$ determines the effect. This may be considered as the quantum mechanical analogue of the classical Kagan-Maksimov model[10]) as also used by Knaap and Beenakker[11]). The fact that the coupling between $\boldsymbol{W}[\boldsymbol{J}]^{(2)}$ and the translational energy transport is indeed negligible, is discussed in the appendix.

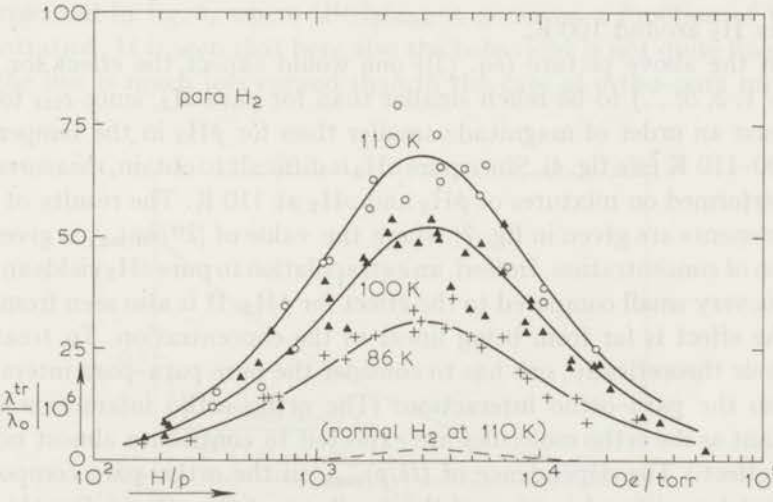

Fig. 5. $|\lambda^{tr}/\lambda_0|$ *vs.* H/p for para H_2 at 86 K, 100 K and 110 K. Pressures between 0.15 and 1 torr.

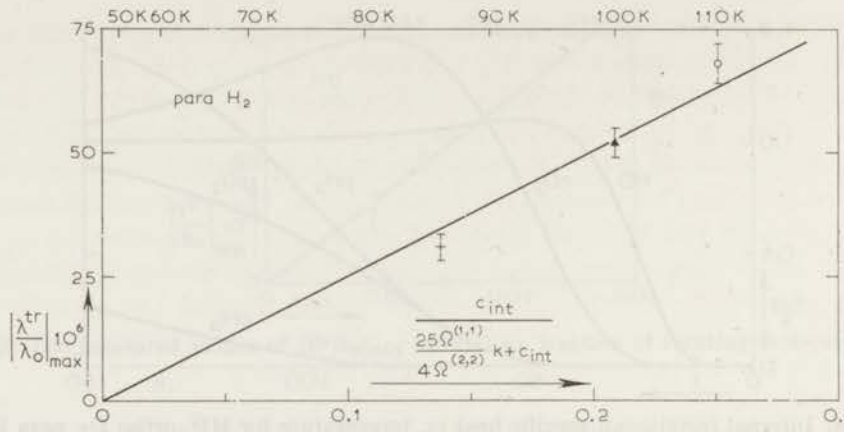

Fig. 6. The measured values of $|\lambda^{tr}/\lambda_0|_{max}$ for para H_2 *vs.* $c_{int}/(25k\Omega^{(1,1)}/4\Omega^{(2,2)} + c_{int})$.

To provide a check on the validity of eq. (3), experiments were performed on para H_2 in the temperature range 85 K–110 K, where c_{int} is strongly temperature dependent (see fig. 4). The results of these measurements are given in fig. 5. The maxima of these curves, being proportional to ψ_{12}, should now be nearly proportional to $c_{int}/(25\ k\Omega^{(1,1)}/4\Omega^{(2,2)} + c_{int})$ (see eq. (3)), if $[^{1200}_{1001}]^2\ [^{1001}_{1001}]^{-1}\ [^{1200}_{1200}]^{-1}_{sph}$ is assumed to be not strongly temperature dependent for p-H_2. A plot based on this assumption is given in fig. 6, and indeed an approximately linear behaviour is found. From the slope of this line it is found that

$$\frac{[^{1200}_{1001}]^2}{[^{1001}_{1001}][^{1200}_{1200}]_{sph}} = 3.5 \times 10^{-4}$$

for para H_2 around 100 K.

From the above picture (eq. (3)) one would expect the effect for ortho $H_2(j = 1, 3, 5, \ldots)$ to be much smaller than for para H_2, since c_{int} for o-H_2 is at least an order of magnitude smaller than for p-H_2 in the temperature range 80–110 K (see fig. 4). Since pure o-H_2 is difficult to obtain, measurements were performed on mixtures of p-H_2 and o-H_2 at 110 K. The results of these measurements are given in fig. 7, where the value of $|\lambda^{tr}/\lambda_0|_{max}$ is given as a function of concentration. Indeed, an extrapolation to pure o-H_2 yields an effect which is very small compared to the effect for p-H_2. It is also seen from fig. 7 that the effect is far from being linear in the concentration. To treat this behaviour theoretically, one has to consider the pure para–para interaction, but also the para–ortho interaction. (The ortho–ortho interaction is less important as the ortho molecules are expected to contribute almost nothing to the effect.) The dependence of $(H/p)_{max}$ on the ortho–para composition could not be analysed in view of the smallness of the effects. For the same reason, mixtures of para H_2 with noble gases were not investigated.

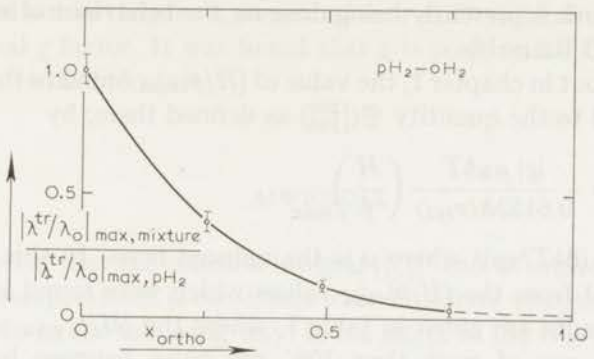

Fig. 7. The behaviour of para H_2–ortho H_2 mixtures: $|\lambda^{tr}/\lambda_0|_{max}$ *vs.* composition at 110 K.

The results obtained for ortho D_2 and normal D_2 can now also be qualitatively understood. For oD_2 ($j = 0, 2, \ldots$) which has an even larger c_{int} than pH_2, one expects an appreciable effect. This is indeed found. For normal D_2, which contains 33% para molecules having a much smaller value of c_{int} (see fig. 4), one expects to find a smaller effect. The values of $|\lambda^{tr}/\lambda_0|_{max}$ for oD_2 and nD_2 differ by almost a factor 3, although nD_2 consists of $\frac{2}{3}$ ortho molecules. This can be understood by assuming that ortho-para mixtures of D_2 behave approximately as do para-ortho mixtures of H_2 (fig. 7). This cannot easily be checked over an extensive concentration range, since for D_2 only the concentration range $\frac{2}{3}$ ortho to pure ortho is easily accessible. However, since the effect is relatively large, mixtures of oD_2 with a noble gas can be investigated. The results of such a study with He are presented in fig. 8, where $|\lambda^{tr}/\lambda_0|_{max}$ is given as a function of the He concentration. It is seen that here also the behaviour is not quite linear, but that the line is much less curved than in the case of ortho–para mixtures.

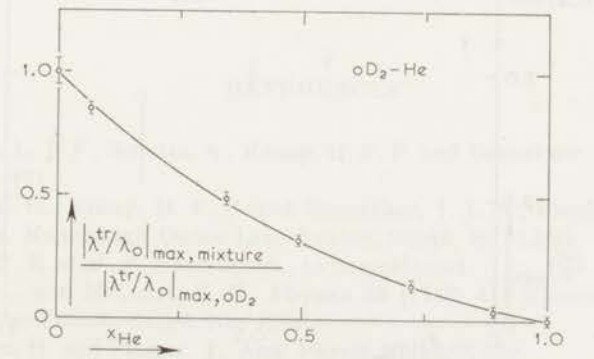

Fig. 8. The behaviour of ortho D_2–He mixtures: $|\lambda^{tr}/\lambda_0|_{max}$ *vs.* composition at 90 K.

Theoretical work is presently being done on the behaviour of such mixtures by Köhler and Raum[12]).

As pointed out in chapter I, the value of $(H/p)_{max}$ found in the experiment can be related to the quantity $\mathcal{S}(^{1200}_{1200})$ as defined there, by

$$\mathcal{S}(^{1200}_{1200}) = \frac{|g|\,\mu_N kT}{0.6153\hbar\langle v_{rel}\rangle}\left(\frac{H}{p}\right)_{max}, \tag{4}$$

with $\langle v_{rel}\rangle = (8kT/\pi\mu)^{\frac{1}{2}}$ where μ is the reduced mass. In this way, $\mathcal{S}(^{1200}_{1200})$ was calculated from the $(H/p)_{max}$ values which were found in the experiment. The results are given in table I, where the $(H/p)_{max}$ values having a measuring error of more than 30% are given between brackets. Also the ratio of the experimental $(H/p)_{max}$ value and the one calculated for the elastic collision model according to eq. (12) of chapter I, is given in table I. This quantity is equal to the ratio of the experimentally determined collision integral and the one calculated for the elastic model where $\boldsymbol{J}$ does not change, neither in magnitude nor in direction. As can be expected for the hydrogen isotopes, where those changes in $\boldsymbol{J}$ are infrequent as is known, *e.g.*, from the acoustical relaxation and the Senftleben–Beenakker effect for the viscosity, this ratio is, within measuring accuracy, equal to unity over the whole temperature range. The value of $\mathcal{S}(^{1200}_{1200})$ has the tendency to decrease with increasing temperature. This tendency is found also for other gases when comparing the low-temperature values with those found at 300 K (see chapter III). The $(H/p)_{max}$ values as found from the measurements on oD$_2$–He mixtures are given in fig. 9. These results can still be reconciled with the expected[15]) linear dependence on composition. The $(H/p)_{max}$ value for pure oD$_2$ seems larger than the $(H/p)_{max}$ as obtained by extrapolation to pure He. This seems to point to a somewhat larger value of $\mathcal{S}$ for the oD$_2$–oD$_2$ interaction than for the oD$_2$–He interaction.

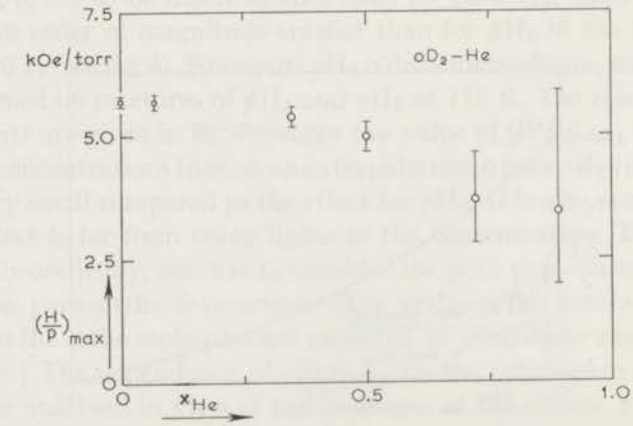

Fig. 9. $(H/p)_{max}$ *vs.* composition for ortho D$_2$–He mixtures at 90 K.

As pointed out in chapter I, measurements of λ^{tr} yield directly the sign of the rotational g factor. It was found that g is positive for H_2, HD and D_2, in agreement with literature.

APPENDIX

The assumption that the collision integral $[{}^{1200}_{1010}]$ can be neglected for H_2 and D_2 at these temperatures is consistent with data from viscosity experiments, as can be seen in the following way. If the effect of the $\boldsymbol{W}[\boldsymbol{J}]^{(2)}$ term on the translational energy transport were considered separately, then instead of eq. (3) one would obtain for ψ_{12} (see also eq. (1)):

$$0.702 \left| \frac{\lambda^{tr}}{\lambda_0} \right|_{max} = \psi_{12} = \tfrac{1}{2} \frac{[{}^{1200}_{1010}]^2}{[{}^{1010}_{1010}][{}^{1200}_{1200}]_{sph}}. \tag{5}$$

Now, use can be made of the relation[13] $[{}^{1200}_{1010}] = \frac{1}{2}[{}^{0200}_{2000}]$, which last collision integral is the decisive bracket for the magnetic field effect on the viscosity[8]):

$$\left(\frac{\Delta\eta_3}{\eta_0} \right)_{sat} = - \frac{[{}^{0200}_{2000}]^2}{[{}^{0200}_{0200}][{}^{2000}_{2000}]}. \tag{6}$$

The diagonal collision integrals $[{}^{1010}_{1010}]$, $[{}^{1200}_{1200}]_{sph}$ and $[{}^{2000}_{2000}]$ are all of the same order of magnitude, since they are connected to the elastic collision cross section, while $[{}^{0200}_{0200}]$ is, for the hydrogen isotopes, an order of magnitude smaller, since it is related to the reorientation cross section. It was found by Korving *et al.*[14]) that $|\Delta\eta_3/\eta_0|_{sat}$ is for para H_2 at room temperature of the order 10^{-5}. From eq. (5) one would thus expect ψ_{12} to be of the order 10^{-6} at room temperature. Since for the contribution considered here, ψ_{12} is proportional to the fraction of rotating molecules, one would expect ψ_{12} to be only of order 10^{-7} at 110 K. Hence, the contribution mentioned in eq. (5) can be neglected for para H_2.

REFERENCES

1) Hermans, L. J. F., Schutte, A., Knaap, H. F. P. and Beenakker, J. J. M., Physica **46** (1970) 491.
2) Sluyter, C. G., Knaap, H. F. P. and Beenakker, J. J. M., Physica **31** (1965) 915 (Commun. Kamerlingh Onnes Lab., Leiden, Suppl. No. 123*a*).
3) Köhler, W. E. *et al.*, Z. Naturforsch., to be published.
4) Levi, A. C. and McCourt, F. R., Physica **38** (1968) 415 (Commun. Kamerlingh Onnes Lab., Leiden, Suppl. No. 126*a*).
5) Senftleben, H. and Piezner, J., Ann. Physik **30** (1937) 541.
6) Heemskerk, J. P. J. *et al.*, to be published.

7) Hirschfelder, J. O., Curtiss, C. F. and Bird, R. B., The molecular Theory of Gases and Liquids, John Wiley and Sons, Inc. (New York, 1954).
8) Korving, J., Physica **46** (1970) 619 (Commun. Kamerlingh Onnes Lab., Leiden No. 376*d*).
9) Hess, S. and Waldmann, L., Z. Naturforsch. **23a** (1968) 1893.
10) Kagan, Yu. and Maksimov, L., Soviet Physics–JETP **24** (1967) 1272.
11) Knaap, H. F. P. and Beenakker, J. J. M., Physica **33** (1967) 643 (Commun. Kamerlingh Onnes Lab., Leiden, Suppl. No. 124*a*).
12) Köhler, W. E. and Raum, H., Z. Naturforsch., to be published.
13) Levi, A. C., McCourt, F. R. and Beenakker, J. J. M., Physica **42** (1969) 363 (Commun. Kamerlingh Onnes Lab., Leiden, Suppl. No. 126*e*).
14) Korving, J., Hulsman, H., Scoles, G., Knaap, H. F. P. and Beenakker, J. J. M., Physica **36** (1967) 177 (Commun. Kamerlingh Onnes Lab., Leiden No. 357*b*).
15) Tip, A., Physica **37** (1967) 411.

CHAPTER III

THE HEAT CONDUCTIVITY OF POLYATOMIC GASES IN MAGNETIC FIELDS

III. $\lambda^{//}$ AND $\lambda^{\perp}$

Synopsis

Experimental data are presented on the change of the thermal conductivity coefficient, $\Delta\lambda$, of polyatomic gases under the influence of a magnetic field (Senftleben–Beenakker effect) at room temperature. A hot-plate type apparatus which allows measurements with the field oriented both parallel to and perpendicular to the temperature gradient was used. The data for $\Delta\lambda^{//}$ and $\Delta\lambda^{\perp}$ permit an evaluation of the different terms which occur in an expansion (in velocities and angular momenta) of the non-equilibrium distribution function. The gases N_2, CO, HD, H_2, D_2, CH_4, CD_4, CF_4, SF_6 and O_2 were investigated.

1. *Introduction.* In the presence of a magnetic field the heat flux through a polyatomic gas is linked to the temperature gradient by

$$q_i = -\sum_k \lambda_{ik} \frac{\partial T}{\partial x_k}, \tag{1}$$

where q_i is the heat flux in the i-direction and $\partial T/\partial x_k$ the temperature gradient in the k-direction. When space symmetry arguments are applied the tensor λ_{ik} can be shown to take the form

$$\boldsymbol{\lambda} = \begin{pmatrix} \lambda^{//}(H) & 0 & 0 \\ 0 & \lambda^{\perp}(H) & -\lambda^{\mathrm{tr}}(H) \\ 0 & \lambda^{\mathrm{tr}}(H) & \lambda^{\perp}(H) \end{pmatrix}, \tag{2}$$

with $\boldsymbol{H} = (H, 0, 0)$. In the absence of a field $\lambda^{//} = \lambda^{\perp} = \lambda_0$ and $\lambda^{\mathrm{tr}} = 0$. $\lambda^{//}$ and $\lambda^{\perp}$ are even in the field while λ^{tr} is odd. Results for λ^{tr} were given in the previous chapters[1]). On the coefficients $\lambda^{//}$ and $\lambda^{\perp}$ several sets of measurements are by now available in the literature. For a survey of existing data see refs. 2 and 3. Utilizing the already existing data it is, nevertheless, quite difficult to make a thorough comparison between theory and experiment.

This is not entirely due to systematic differences between the results obtained by different authors. Rather, it is in particular due to the fact that accurate measurements of $\Delta\lambda^{//}$ $(=\lambda^{//} - \lambda_0)$, the change in the heat conductivity with the magnetic field parallel to the temperature gradient, could not be performed in the hot-wire apparatus utilized previously. A calculation of $\Delta\lambda^{//}$ from the data for $\Delta\lambda^{\perp}$ and $\frac{1}{2}(\Delta\lambda^{\perp} + \Delta\lambda^{//})$, both measured with hot-wire apparatus but under quite different experimental conditions, is not sufficiently reliable for a useful comparison with theory; this will become clearer later in this work.

The unavailability of reliable data for $\Delta\lambda^{//}$ and $\Delta\lambda^{\perp}$ can be overcome by using a hot-plate type apparatus in which these quantities can be directly measured under the same experimental conditions. A previous attempt to construct an apparatus of this type was undertaken by Senftleben in 1936[4]). He approximated a hot plate with a set of parallel platinum wires and using this apparatus, he obtained data for O_2 with a claimed accuracy of $\pm 10\%$. It is the purpose of this work to present room temperature data on both $\Delta\lambda^{//}$ and $\Delta\lambda^{\perp}$ obtained in an apparatus of the hot-plate type, this apparatus having a sensitivity (in $\Delta\lambda/\lambda$) of 5 parts in 10^6. Moreover, the relatively large dimensions of the apparatus allow measurements at low pressures without having large Knudsen corrections. Consequently, high values of the ratio of field to pressure, H/p, can be reached so that, for most gases, the curves for $\Delta\lambda^{//}/\lambda$ and $\Delta\lambda^{\perp}/\lambda$ as a function of H/p can be measured easily into the saturation region (see, *e.g.*, fig. 7).

2. *Apparatus.* 2*a.* General. A schematic diagram of the experimental arrangement is given in fig. 1. The apparatus consists of two cylindrical cells, placed between two parallel brass plates held at the same temperature. One of the cells contains the gas to be investigated while the other cell, serving as a reference cell, can be filled with a noble gas. Both cells are surrounded by a vacuum jacket. Halfway along each cell there is a thin plate which serves as the hot plate and which divides the cell into two equal parts. This plate is, however, only spot-connected so that the pressure in both halves of the cell is equalized. A temperature gradient is directed along the axes of the cells by applying a constant heat input to the center plates. The magnetic field can be applied either parallel to or perpendicular to this temperature gradient by orienting a magnet appropriately. In this way, both $\Delta\lambda^{//}$ and $\Delta\lambda^{\perp}$ are measured by observing the change, $\delta T(\boldsymbol{H})$, in the temperature of the hot plate in the sample cell.

In the measuring and reference cells, the temperatures of the hot plates are measured with thermistors R_m and R_r, respectively. The common temperature of the cold plates is measured with thermistor R_c. The applied temperature difference $\Delta T(\approx 10\ \mathrm{K})$ is derived from the resistances of the thermistors. On the other hand, the temperature change $\delta T(\boldsymbol{H})$ is measured

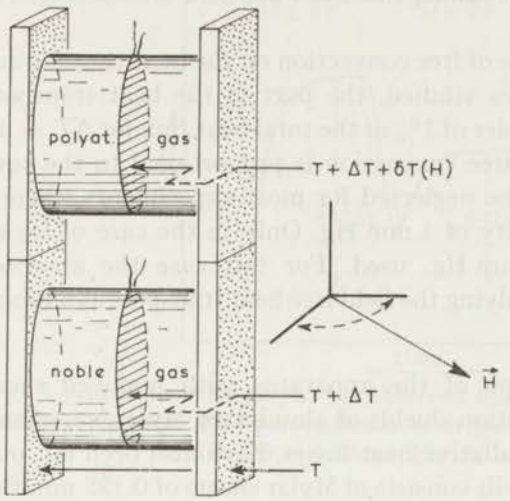

Fig. 1

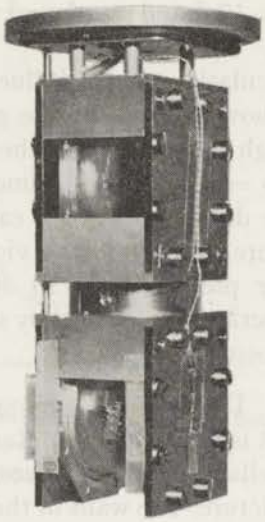

Fig. 2

Fig. 1. Schematic diagram of the apparatus.

Fig. 2. Photograph of the apparatus with radiation shields and vacuum jacket removed.

directly in a Wheatstone bridge arrangement with the thermistors R_m and R_c. A higher sensitivity, if needed, is obtained by measuring R_m differentially against R_r, which itself remains at constant temperature since the thermal conductivity of the noble gas is not affected by the field. In this way, with one exception, all spurious effects cancel out within the measuring accuracy. The aforementioned exception is due to the imperfect matching of the field effects on the resistance of the thermistors, thereby resulting in very small corrections at the highest field strengths. A possible change in the heat input, due to the magnetic field affecting the resistance of the heater, was avoided by having a second resistance in the constant voltage heating circuit, equal to that of the heater, but outside the field. In this way, small variations in the resistance of the heater do not affect the heat input in first order. Furthermore, having a constant heat input, small displacements of the hot plate under influence of Lorentz forces affect ΔT only in second order, because of the symmetry of the two cell halves. Thus, the hot plates could be constructed from a very thin and light weight material in order to obtain a short response time.

Experiments with noble gases in both cells at different values of ΔT have conclusively demonstrated that the only spurious effect not eliminated by the above-described precautions was the aforementioned influence of the high fields on the thermistors. The maximum unbalance of the bridge circuit produced in this way (at 23 kOe) corresponded to an effect in $\Delta\lambda/\lambda$

of 3×10^{-5} and was found to be independent of the field orientation in this setup.

Calculations on the influence of free convection on the heat transfer in the cell showed that, for the gases studied, the part of the heat transported through convection is of the order of 1% of the total heat flux for $\Delta T = 10$ K and $p = 50$ mm Hg[5]). Since free convection is proportional to the square of the density, its effect can be neglected for most experiments where the pressure range is in the vicinity of 1 mm Hg. Only in the case of O_2 were higher pressures, up to 30 mm Hg, used. For this case the absence of convection was verified by studying the field free heat transport as a function of pressure.

2*b*. Details. A photograph of the apparatus with removed vacuum jacket is given in fig. 2. Radiation shields of aluminized Mylar, surrounding the cells in order to reduce radiative heat losses, have also been left out of the picture. The walls of the cells consists of Mylar sheets of 0.125 mm thickness, made into a cylinder by melting two sides together with a hot wire. The seams were covered with a thin layer of Araldite (epoxy resin) to ensure vacuum-tightness. The inner diameter of the cells is 34.0 mm while the total length is 20.0 mm (the distance between a hot plate and either cold plate is 9.8 mm). The connections between cylinders and brass plates were made using an indium "O"-ring construction, in essence similar to that described in chapter I, where the same procedure has proven useful even at low temperature. The brass plates were given a chromium coating in order to reduce radiative heat losses.

The hot plates consist of a 0.2 mm thick Mylar frame in the center of which a thermistor is inserted and upon which the heater is wound (0.05 mm constantan wire, total resistance 405 Ω). The distance between the windings is 1 mm. A cover of aluminum foil (0.01 mm) assures temperature homogeneity throughout the plate and simultaneously reduces radiative heat losses. That part of the electrical circuit which passes from the hot to the cold plates was provided by a very thin (0.03 mm) copper wire. In addition, the effect of the Lorentz force on the wires is avoided by twisting together each pair. The thermistors used are of the type Philips B 8 32003 P/22k with the glass covers removed. Their resistance at 293 K is approximately 25 kΩ, the temperature coefficient -4.5% K^{-1}. As a null instrument in the bridge circuit, a Keithley microvoltmeter (model 150) was used in combination with a chart recorder. A temperature resolution of 3×10^{-5} K was achieved. Good temperature stability of the apparatus as a whole was obtained by having a long response time to fluctuations in the temperature of the bath; this was achieved by combining the large heat capacity of the apparatus and relatively poor thermal contact with the bath (see fig. 2). Fluctuations of ± 20 mK which occurred in the waterbath when it was fed by an ordinary

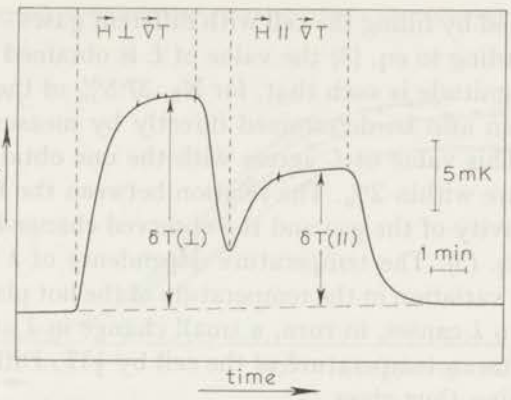

Fig. 3. A typical recorder graph: the observed temperature change in the hot plate caused by a magnetic field perpendicular to or parallel to the gradient.
(HD, $p = 1.27$ mm Hg, $H = 16.8$ kOe.)

circulating water thermostat were thus reduced by a factor 20. However, the best stability was reached in a non-circulating water bath in a glass dewar. In this case, special measures had to be taken in order to avoid convection in the bath caused by the rather large energy release from the apparatus (up to 0.7 W). This was achieved by surrounding the vacuum jacket by a 0.6 mm thick copper shield, by which the dissipated heat was distributed to the bath over a vertical range of 40 cm. Moreover, a spongy material was placed on top of the vacuum jacket at the point where the heat is released. Thus the effect of the temperature fluctuations on the temperature difference between the two hot plates was reduced to 3×10^{-5} K. The slow temperature rise of the non-circulating waterbath manifests itself as a slight drift on the recorder chart (see fig. 3). This does, however, not reduce the temperature resolution mentioned above.

3. *Calculation of the results.* At a fixed pressure of the gas in the measuring cell experiments were performed at several field strengths. Every measurement was carried out with the field directed both in the parallel and the perpendicular orientation. A typical recorder graph is shown in fig. 3. The quantity $\Delta\lambda^{\perp}/\Delta\lambda^{//}$ is found directly from the ratio of the deflections on the recorder chart (only at the highest fields the above mentioned small correction for the field effect on the thermistors has to be applied). For a calculation of $\Delta\lambda/\lambda$ from the recorder deflections, the total heat flow through the cell is written as

$$Q = (A\lambda + L)\,\Delta T, \tag{3}$$

where A represents a geometric factor for the cell, and L accounts for the heat leaks through radiation, wall and electrical leads. By plotting the values

of $Q/\Delta T$ – obtained by filling the cell with different gases – *vs.* the literature values of λ, according to eq. (3) the value of L is obtained by extrapolating to $\lambda = 0$. Its magnitude is such that, for N_2, 37.5% of the total heat input leaks away. L can also be determined directly by measuring $Q/\Delta T$ in the evacuated cell. This value of L agrees with the one obtained in the extrapolation procedure within 2%. The relation between the field effect on the thermal conductivity of the gas and the observed change in ΔT is found by differentiating eq. (3). The temperature dependence of λ and L cannot be neglected since a variation in the temperature of the hot plate by δT through the field effect on λ causes, in turn, a small change in λ and L through the variation in the mean temperature of the cell by $\frac{1}{2}\delta T$. Differentiation of eq. (3) and rearranging thus gives

$$\frac{\delta Q}{Q} = \frac{\delta\lambda(\boldsymbol{H})}{\lambda}\left(\frac{1}{1 + L/A\lambda}\right) + \frac{\delta T}{\Delta T}(1 + \tfrac{1}{2}\alpha\Delta T), \tag{4}$$

where $\delta\lambda(\boldsymbol{H})$ is the field effect on λ, and

$$\alpha = \left(\frac{A\lambda}{A\lambda + L}\right)\frac{1}{\lambda}\frac{\partial\lambda}{\partial T} + \left(\frac{L}{A\lambda + L}\right)\frac{1}{L}\frac{\partial L}{\partial T}. \tag{5}$$

Since Q is kept constant in the experiment, the left-hand side of eq. (4) vanishes and $\delta\lambda(\boldsymbol{H})/\lambda$ can be calculated from

$$\frac{\delta\lambda(\boldsymbol{H})}{\lambda} = -\frac{\delta T}{\Delta T}\left(1 + \frac{L}{A\lambda}\right)(1 + \tfrac{1}{2}\alpha\Delta T). \tag{6}$$

For all gases, the correction term $\frac{1}{2}\alpha\Delta T$ can be calculated to be less than 0.04 for $\Delta T = 10$ K and $(1/L)(\partial L/\partial T) = 0.01$ K^{-1} (the value appropriate to radiation at room temperature, the main contribution in L). Using the calibration of the thermistors, δT is found from the unbalance of the Wheatstone bridge. An independent calibration of the recorder deflection in terms of $\delta T/\Delta T$ can be obtained by varying Q by a specified amount in the absence of a field. It is seen (eq. (4) with $\delta\lambda(\boldsymbol{H}) = 0$) that $\delta Q/Q$ should then be equal to $\delta T/\Delta T$ apart from the small correction $\frac{1}{2}\alpha\Delta T$. Using the calculated value for α the two calibrations were found to agree within 1% for all gases.

The results of some measurements for N_2 as calculated using formula (6) are given in fig. 4. As found earlier theoretically as well as experimentally, the observed effect should be a unique function of the ratio of field to pressure, H/p, since it depends on the parameter $\omega_p\tau$ where ω_p ($\sim H$) is the precession frequency of the angular momentum of the molecule around the field direction, and τ ($\sim 1/p$) is the relevant time scale, of the order of the mean free flight time between two collisions. However, it can be seen from fig. 4 that $\delta\lambda/\lambda$ is not a unique function of H/p, and that small deviations occur

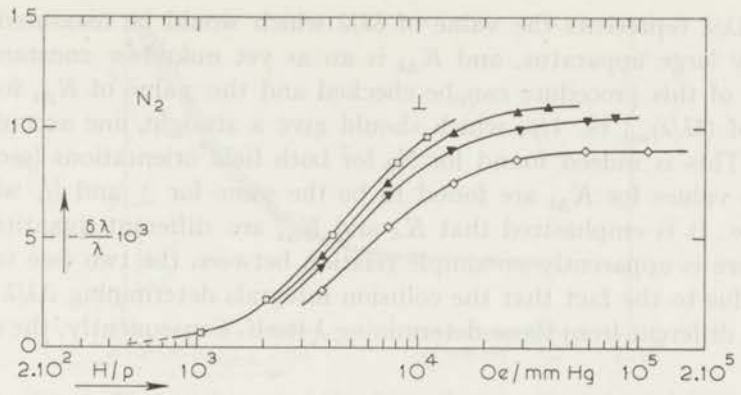

Fig. 4. The observed field effect on λ without the application of Knudsen corrections, as calculated using eq. (6).

□ $p = 2.09$ mm Hg ▼ $p = 0.283$ mm Hg
▲ $p = 0.59$ mm Hg ◇ $p = 0.153$ mm Hg.

at lower pressures. As found also by other aurhors[6, 7, 8]), the curves at low pressures undergo a reduction in the magnitude of the effect due to the occurrence of Knudsen effects. In a manner analogous to that in which the Knudsen correction K_λ for the field free thermal conductivity coefficient appears, *viz.*, where λ is given by

$$\lambda = \lambda_{\text{measured}}\,(1 + K_\lambda/p), \tag{7}$$

it is assumed that

$$\frac{\Delta\lambda}{\lambda} = \frac{\delta\lambda}{\lambda}\,(1 + K_{\Delta\lambda}/p), \tag{8}$$

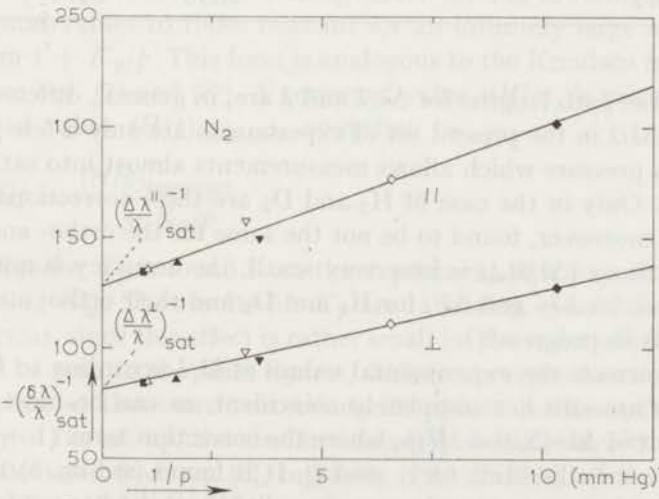

Fig. 5. Determination of the Knudsen correction $K_{\Delta\lambda}$ (see eq. (8)): the inverse of the saturation values of $\delta\lambda^{\perp}/\lambda$ and $\delta\lambda^{\parallel}/\lambda$ *versus* the inverse of the pressure for N_2.

where $\Delta\lambda/\lambda$ represents the value of $\delta\lambda/\lambda$ which would be measured in an infinitely large apparatus, and $K_{\Delta\lambda}$ is an as yet unknown constant. The validity of this procedure can be checked and the value of $K_{\Delta\lambda}$ found in a plot of $(\delta\lambda/\lambda)_{\text{sat}}^{-1}$ *vs.* $1/p$, which should give a straight line according to eq. (8). This is indeed found for N_2 for both field orientations (see fig. 5) and the values for $K_{\Delta\lambda}$ are found to be the same for $\perp$ and //, which is plausible. It is emphasized that K_λ and $K_{\Delta\lambda}$ are different quantities and that there is apparently no simple relation between the two (see table I). This is due to the fact that the collision integrals determining $\Delta\lambda/\lambda$ are, in general, different from those determining λ itself. Consequently, the characteristic mean free path lengths for $\Delta\lambda/\lambda$ and λ are, in general, different. The corrections on $\delta\lambda/\lambda$ in the present set of experiments are only a few percent at 1 mm Hg, a pressure which allows measurements almost into saturation for most gases. Only in the case of H_2 and D_2 are these corrections rather large, and are, moreover, found to be not the same for the ortho- and para-modifications. Since $(\Delta\lambda/\lambda)_{\text{sat}}$ is here very small, the accuracy is not great. Theoretical work on $\Delta\lambda^\perp$ and $\Delta\lambda^{//}$ for H_2 and D_2 and their ortho- and para-modifications is in progress[9]).

TABLE I

The Knudsen corrections for λ, $\Delta\lambda$ and H/p, and the thermal conductivity coefficient as found in the experiment

	K_λ (mm Hg)	$K_{\Delta\lambda}$ (mm Hg)	K_p (mm Hg)	λ_{exp} (mW/cm K)	λ_{lit} (300 K) (mW/cm K)
N_2	0.030	0.055	0.02	0.268	0.260[10])
CO	0.034	0.028	0.01	0.260	0.252[10])
HD	0.152	0.18	0.09	1.553	1.538 (296.8 K)[11])
n–H_2	0.254	0.8	—	1.884	1.815[10])
p–H_2	0.262	0.4	—	1.940	
n–D_2	0.181	0.16	—	1.360	1.406[10])
o–D_2	0.183	0.32	—	1.364	
CH_4	0.038	0.021	0.02[5]	0.366	0.343[10])
CD_4	0.037	0.014	0.02	0.367	0.347[5 14])
CF_4	0.034	—	—	0.168	
SF_6	0.021	0.004	—	0.136	0.141 (303 K)[15])
O_2	0.040	—	—	0.273	0.274[10])

If one now corrects the experimental values of $\delta\lambda/\lambda$ according to formula (8), the curves are still not completely coincident, as can be most clearly seen from a plot of $\Delta\lambda^\perp/\Delta\lambda^{//}$ *vs.* H/p, where the correction term $(1 + K_{\Delta\lambda}/p)$ drops out since it is the same for $\perp$ and //. It is found (see fig. 6) that for lower pressures, the experimental curves are slightly shifted towards higher H/p values. The origin of this effect on the H/p values is to be found in the

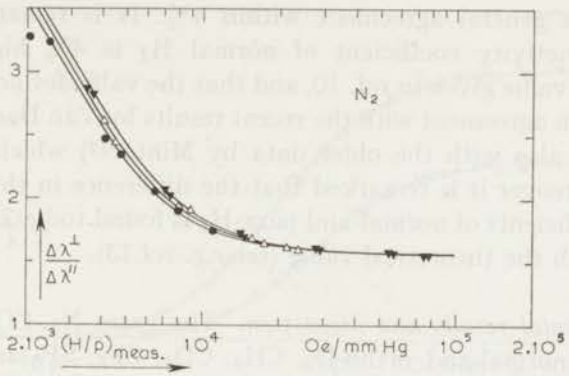

Fig. 6. The appearance of Knudsen effects on the values of H/p: $\Delta\lambda^{\perp}/\Delta^{//}$ *versus* $(H/p)_{\text{measured}}$ for N_2.
● p = 3.51 and 2.09 mm Hg
△ p = 1.07 and 0.96 mm Hg
▼ p = 0.307 and 0.283 mm Hg.

fact that collisions of the molecules with the walls of the apparatus do affect the free flight time τ. At higher pressures, where the mean free path is much shorter than the dimensions of the apparatus, collisions with the wall are relatively scarce, and τ can be taken to be proportional to $1/p$. At lower pressures, however, collisions with the wall become relatively more frequent, thus causing a mean free flight time which is no longer inversely proportional to the pressure. As the effective free flight time thus becomes shorter, the effective value of $\omega_p\tau$ is lower than the one derived from field and pressure. By partitioning the total number of collisions in the gas into a sum of gas–gas and gas–wall collisions, the scaling factor for the lowering of the H/p experimental values to those relevant for an infinitely large apparatus takes the form $1 + K_p/p$. This form is analogous to the Knudsen factors for λ and $\Delta\lambda/\lambda$ (see eqs. (7) and (8)). A corrected value, (H/p), is calculated from the measured value, $(H/p)_{\text{measured}}$, according to

$$H/p = \frac{(H/p)_{\text{measured}}}{1 + K_p/p}. \tag{9}$$

The value for K_p is found from the experiment in a way analogous to that for finding $K_{\Delta\lambda}$. The results for K_p are tabulated in table I. The accuracy is not great, since this effect is rather small (of the order of 1% at 1 mm Hg). As will be seen in the final figures, $\Delta\lambda/\lambda$ is a unique function of H/p after application of these two corrections. As a last check on the general consistency of the set-up, the absolute values of λ as found with this apparatus were calculated from eq. (3), replacing A by $2\pi R^2/d$, where R is the radius of the cells and d is the distance between hot and cold plate. These results are also given in table I. A comparison of these data with existing literature

values gives a general agreement within 4%. It is remarked, that the thermal conductivity coefficient of normal H_2 is 4% higher than the recommended value given in ref. 10, and that the value for normal D_2 is 3% lower. This is in agreement with the recent results by Van Dael and Cauwenbergh[11]), and also with the older data by Minter[12]) which are not used in ref. 10. Moreover it is remarked that the difference in the thermal-conductivity coefficients of normal-and para-H_2 is found to be 2.9%, in perfect agreement with the theoretical value (see *e.g.* ref.13).

4. *Experimental results and discussion.* The gases N_2, CO, HD, normal- and para-H_2, normal-and ortho-D_2, CH_4, CD_4, CF_4, SF_6 and O_2 were investigated (see figs. 7–18). The purity of these gases was better than 99% with the exception of CD_4, which was investigated in two samples, containing 5% and 9% CHD_3. Since the results for these two samples do not differ beyond measuring accuracy (see fig. 15), it can be assumed that the same result would be found for pure CD_4. The hydrogen isotopes H_2 and D_2, which show extremely small effects, were verified to contain as little as 1×10^{-4} of non-isotopic impurities. For N_2, measurements were performed both with $\Delta T = 10$ K and with $\Delta T = 2$ K to have a check on the validity of eq. (6). A good agreement between the two results is found (see fig. 7).

In table II all characteristic quantities following from the present measurements are given. The accuracy in the ratio $(\Delta\lambda^{\perp}/\Delta\lambda^{//})_{sat}$, which is directly measured, is, for most gases, as good as $\pm$ 1%. This can be seen in fig. 19 where the direct results of $\Delta\lambda^{\perp}/\Delta\lambda^{//}$ *vs.* H/p are given for N_2, CO and CH_4.

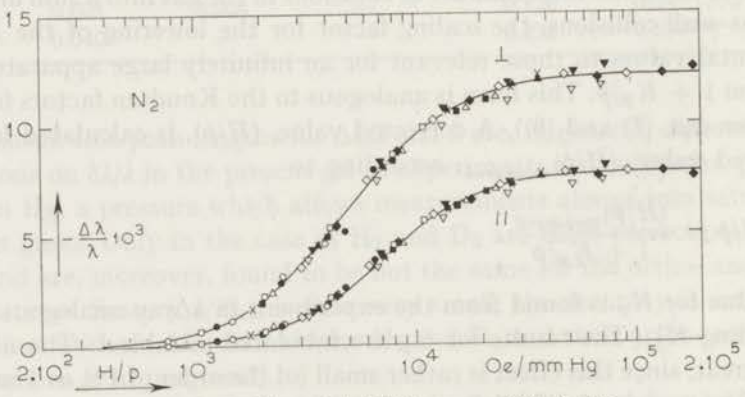

Fig. 7. $(\Delta\lambda^{\perp}/\lambda)$ and $(\Delta\lambda^{//}/\lambda)$ *versus* H/p for N_2.

○ $p = 6.80$ mm Hg	▲ $p = 0.59$ mm Hg
● $p = 3.51$ mm Hg	▽ $p = 0.307$ mm Hg
□ $p = 2.09$ mm Hg	▼ $p = 0.283$ mm Hg
■ $p = 1.07$ mm Hg	◇ $p = 0.153$ mm Hg
△ $p = 0.96$ mm Hg	◆ $p = 0.097$ mm Hg

× $p = 0.59$ mm Hg and $\Delta T = 2$K.

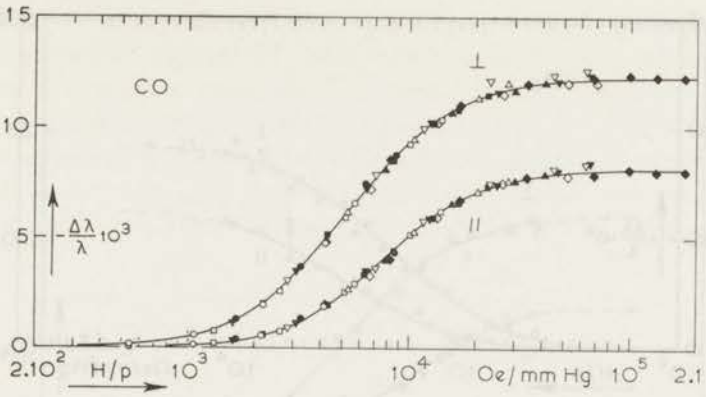

Fig. 8. $(\Delta\lambda^{\perp}/\lambda)$ and $(\Delta\lambda^{\parallel}/\lambda)$ *versus* H/p for CO.

○ $p = 4.03$ mm Hg ▲ $p = 0.53$ mm Hg
● $p = 2.65$ mm Hg ▽ $p = 0.36$ mm Hg
□ $p = 1.65$ mm Hg ▼ $p = 0.33$ mm Hg
■ $p = 0.99^5$ mm Hg ◇ $p = 0.314$ mm Hg
△ $p = 0.81$ mm Hg ◆ $p = 0.114$ mm Hg.

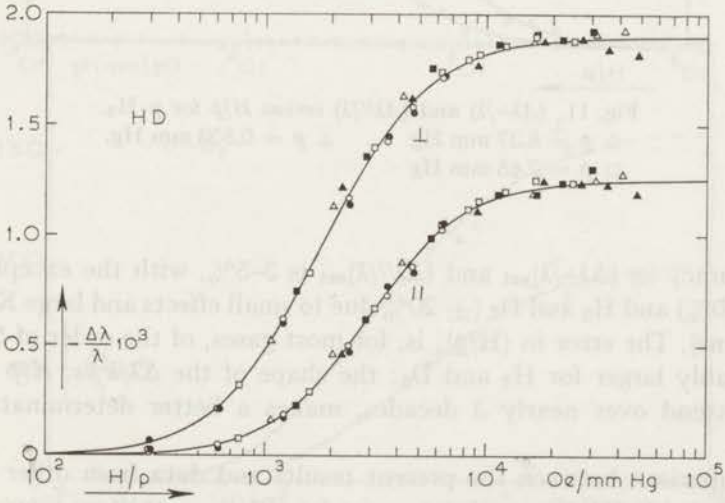

Fig. 9. $(\Delta\lambda^{\perp}/\lambda)$ and $(\Delta\lambda^{\parallel}/\lambda)$ *versus* H/p for HD.

○ $p = 3.49$ mm Hg ■ $p = 0.65$ mm Hg
● $p = 3.47$ mm Hg △ $p = 0.40$ mm Hg
□ $p = 1.27$ mm Hg ▲ $p = 0.35$ mm Hg.

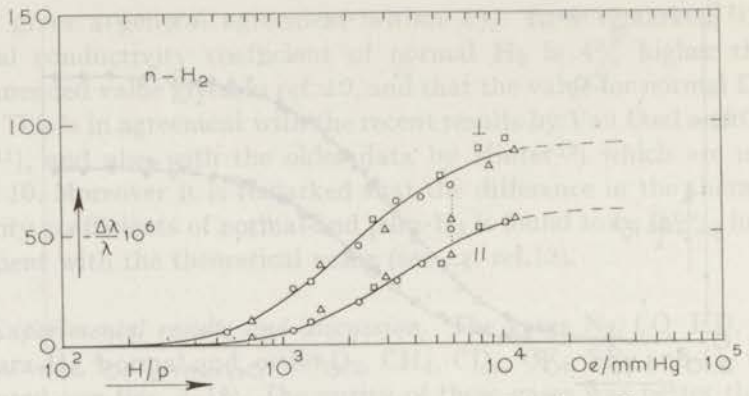

Fig. 10. $(\Delta\lambda^{\perp}/\lambda)$ and $(\Delta\lambda^{//}/\lambda)$ *versus* H/p for n–H_2.
○ $p = 3.88$ mm Hg △ $p = 1.47$ mm Hg.
□ $p = 1.63$ mm Hg

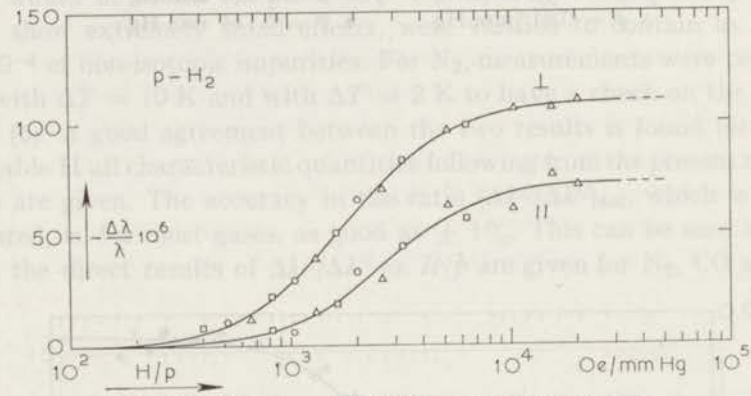

Fig. 11. $(\Delta\lambda^{\perp}/\lambda)$ and $(\Delta\lambda^{//}/\lambda)$ *versus* H/p for p–H_2.
○ $p = 8.37$ mm Hg △ $p = 0.833$ mm Hg.
□ $p = 2.65$ mm Hg

The accuracy in $(\Delta\lambda^{\perp}/\lambda)_{sat}$ and $(\Delta\lambda^{//}/\lambda)_{sat}$ is 3–5%, with the exceptions of SF_6($\pm$ 10%) and H_2 and D_2 ($\pm$ 20% due to small effects and large Knudsen corrections). The error in $(H/p)_{\frac{1}{2}}$ is, for most gases, of the order of 5% and considerably larger for H_2 and D_2: the shape of the $\Delta\lambda/\lambda$ *vs.* H/p curves, which extend over nearly 3 decades, makes a better determination impossible.

A comparison between the present results and data from other sources is made in table III. Since no data exist for $(\lambda^{tr}/\lambda)_{max}$ at room temperature, the comparison is confined to the values of $(\Delta\lambda^{\perp}/\lambda)_{sat}$ and $(\Delta\lambda^{//}/\lambda)_{sat}$, and the combination $[\frac{1}{2}(\Delta\lambda^{\perp} + \Delta\lambda^{//})/\lambda]_{sat}$, as measured by other authors. For purposes of comparison the present results of $\Delta\lambda^{\perp}$ and $\Delta\lambda^{//}$ have been com-

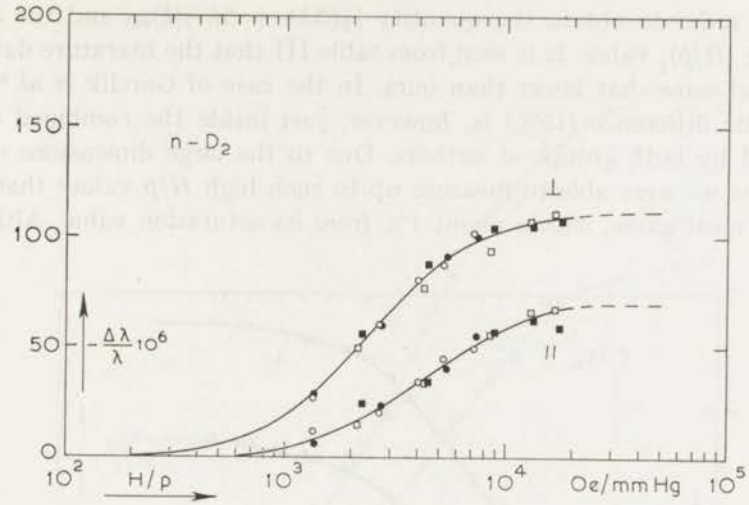

Fig. 12. $(\Delta\lambda^{\perp}/\lambda)$ and $(\Delta\lambda^{//}/\lambda)$ *versus* H/p for n–D_2.
○ $p = 3.20$ mm Hg □ $p = 1.01$ mm Hg
● $p = 3.11$ mm Hg ■ $p = 0.97$ mm Hg.

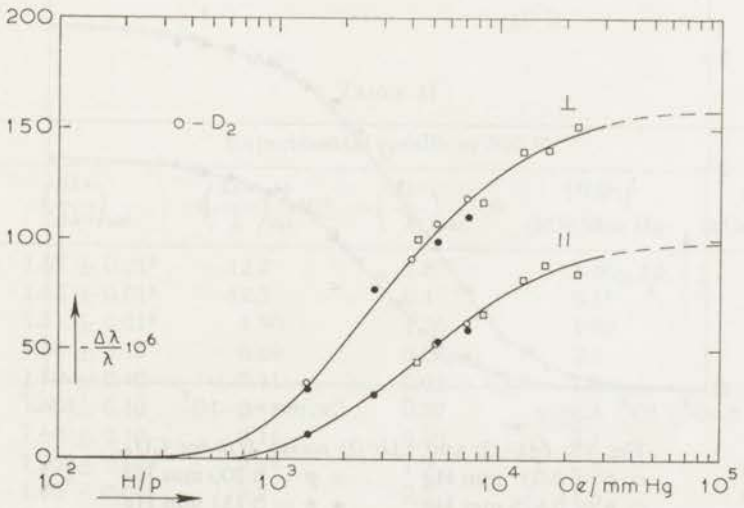

Fig. 13. $(\Delta\lambda^{\perp}/\lambda)$ and $(\Delta\lambda^{//}/\lambda)$ *versus* H/p for o–D_2.
○ $p = 3.20$ mm Hg □ $p = 1.01$ mm Hg.
● $p = 3.16$ mm Hg

bined in order to obtain the quantity $[\frac{1}{2}(\Delta\lambda^{\perp} + \Delta\lambda^{//})/\lambda]_{sat}$ and the corresponding $(H/p)_{\frac{1}{2}}$ value. It is seen from table III that the literature data are in general somewhat lower than ours. In the case of Gorelik *et al.*[8]) this systematic difference (15%) is, however, just inside the combined errors indicated by both groups of authors. Due to the large dimensions of our apparatus we were able to measure up to such high H/p values that $\Delta\lambda/\lambda$ was, for most gases, within about 1% from its saturation value. Although

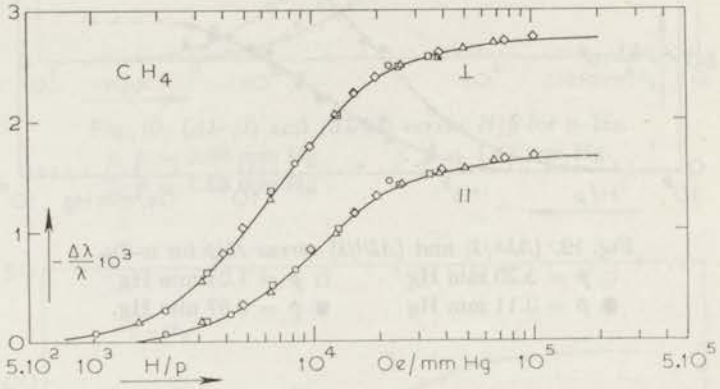

Fig. 14. $(\Delta\lambda^{\perp}/\lambda)$ and $(\Delta\lambda^{//}/\lambda)$ *versus* H/p for CH_4.
○ p = 1.01 mm Hg △ p = 0.318 mm Hg
□ p = 0.646 mm Hg ◇ p = 0.199 mm Hg.

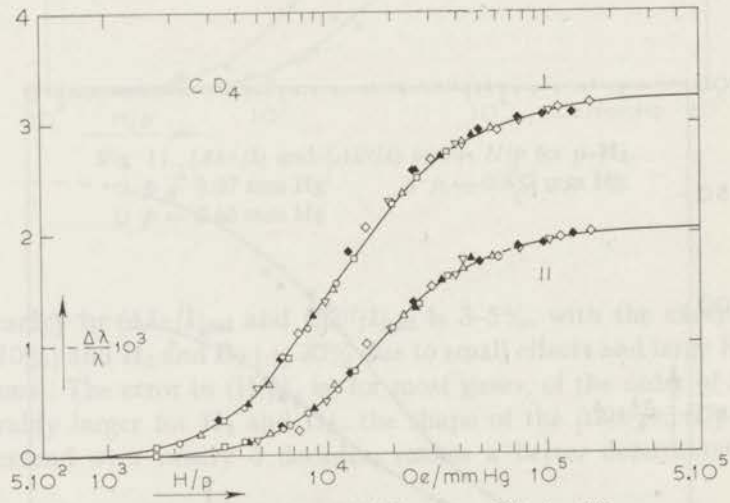

Fig. 15. $(\Delta\lambda^{\perp}/\lambda)$ and $(\Delta\lambda^{//}/\lambda)$ *versus* H/p for CD_4.
○ p = 2.03 mm Hg ▽ p = 0.200 mm Hg
□ p = 0.625 mm Hg ◆ p = 0.151 mm Hg
▲ p = 0.48 mm Hg ◇ p = 0.121 mm Hg.
△ p = 0.383 mm Hg
White symbols: 9% CHD_3; black symbols: 5% CHD_3.

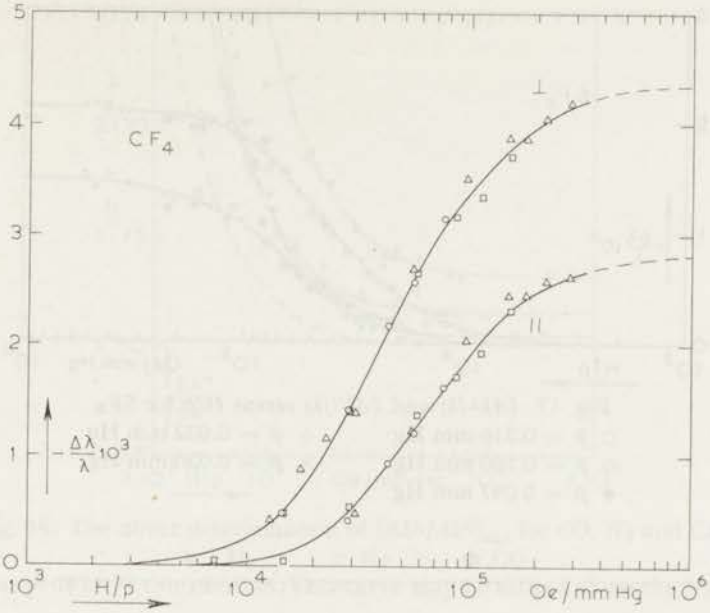

Fig. 16. $(\Delta\lambda^{\perp}/\lambda)$ and $(\Delta\lambda^{//}/\lambda)$ *versus* H/p for CF_4.
○ $p = 0.30$ mm Hg △ $p = 0.072$–0.102 mm Hg.
□ $p = 0.15$ mm Hg

TABLE II

Experimental results at 300 K					
	$\left(\frac{\Delta\lambda^{\perp}}{\Delta\lambda^{//}}\right)_{sat}$	$-\left(\frac{\Delta\lambda^{\perp}}{\lambda}\right)_{sat}10^3$	$-\left(\frac{\Delta\lambda^{//}}{\lambda}\right)_{sat}10^3$	$(H/p)_{\frac{1}{2}}^{\perp}$ (kOe/mm Hg)	$(H/p)_{\frac{1}{2}}^{//}$ (kOe/mm Hg)
N_2	1.57 ± 0.01[5]	12.2	7.8	4.8	7.0
CO	1.52 ± 0.01[5]	12.3	8.1	5.1[5]	7.7
HD	1.51 ± 0.01[5]	1.90	1.26	1.80	2.95
n–H_2	1.50 ± 0.15	0.09	0.06	2.1	3.3
p–H_2	1.50 ± 0.10	0.11	0.07	1.8	2.7
n–D_2	1.60 ± 0.10	0.11	0.07	2.4	4.3
o–D_2	1.60 ± 0.10	0.16	0.10	3.1	4.8
CH_4	1.65[5] ± 0.01[5]	2.7[5]	1.7	6.8	10.5
CD_4	1.60 ± 0.01[5]	3.2	2.0	11.5	17.5
CF_4	1.53 ± 0.02[5]	4.3[5]	2.8	43	65
SF_6	1.45 ± 0.04	2.1	1.4[5]	42.[5]	64
O_2	1.51 ± 0.03	12.6	8.3	0.0093	0.014

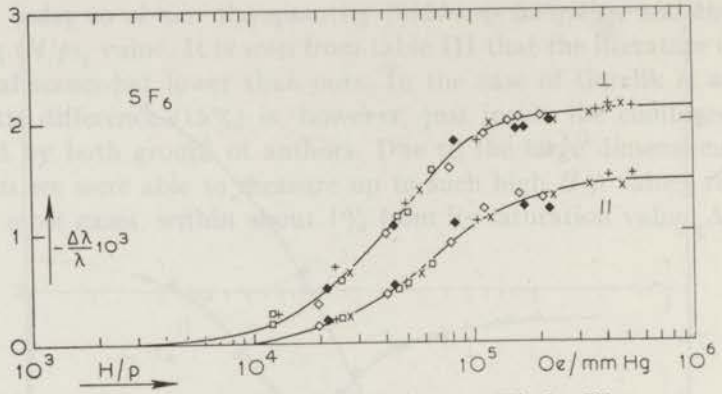

Fig. 17. $(\Delta\lambda^{\perp}/\lambda)$ and $(\Delta\lambda^{\parallel}/\lambda)$ *versus* H/p for SF_6.
□ $p = 0.316$ mm Hg + $p = 0.032$ mm Hg
◇ $p = 0.100$ mm Hg × $p = 0.030$ mm Hg.
◆ $p = 0.097$ mm Hg

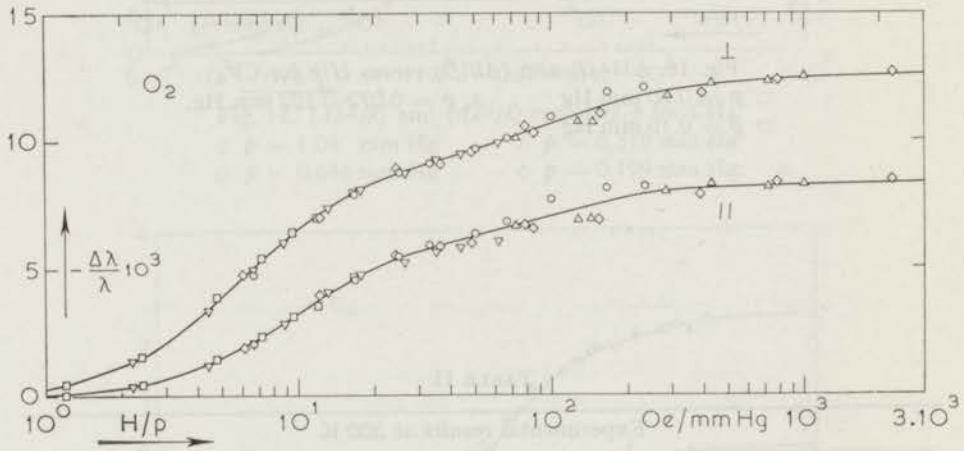

Fig. 18. $(\Delta\lambda^{\perp}/\lambda)$ and $(\Delta\lambda^{\parallel}/\lambda)$ *versus* H/p for O_2.
○ $p = 29.9$ mm Hg ▽ $p = 5.62$ mm Hg
□ $p = 20.8$ mm Hg ◇ $p = 4.07$ mm Hg.
△ $p = 6.98$ mm Hg

the measurements of Gorelik *et al.* reach only about 80% of the saturation value, this is not likely to explain the full discrepancies between their results and ours, as it is possible to extrapolate confidently to full saturation. Their $(H/p)_{\frac{1}{2}}$ values are, however, significantly higher than ours, especially for N_2 and CO, which are rather accurately measurable. This may be caused by the fact that the H/p values in their measurements, which were performed at fairly low pressures, are also affected by Knudsen effects (see eq. (9)).

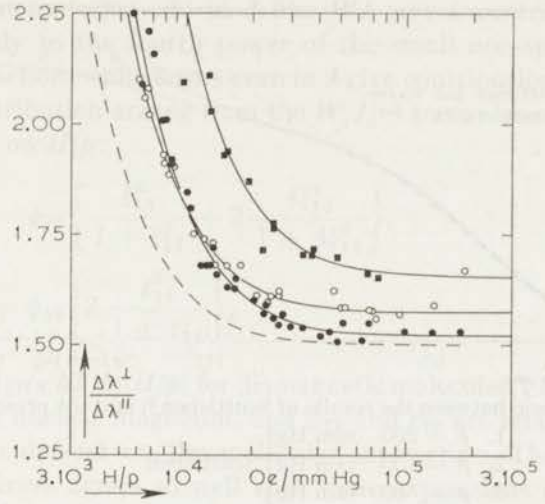

Fig. 19. The direct determination of $(\Delta\lambda^{\perp}/\Delta\lambda^{//})_{sat}$ for CO, N_2 and CH_4.
■ CH_4 ○ N_2 ● CO
----- Theory: $\boldsymbol{W}[\boldsymbol{J}]^{(2)}$ contribution. This curve may be shifted along the H/p axis.

TABLE III

Comparison with literature data

	Measured quantity	Author	$-10^3\left(\frac{\Delta\lambda}{\lambda}\right)_{sat}$		$\left(\frac{H}{p}\right)_{\frac{1}{2}}$ (kOe/mm Hg)	
			literature	this exp.	literature	this exp.
N_2	$\Delta\lambda^{\perp}$	Gorelik *et al.*[8])	10.5	12.2	6.4	4.8
	$\frac{1}{2}(\Delta\lambda^{\perp}+\Delta\lambda^{//})$	Korving *et al.*[7])	7.9	10.0	5.3	5.7
CO	$\Delta\lambda^{\perp}$	Gorelik *et al.*[8])	10.5	12.3	8.3	5.1
	$\frac{1}{2}(\Delta\lambda^{\perp}+\Delta\lambda^{//})$	Korving *et al.*[7])	8.2	10.2	6.9	6.1
n–H_2	$\Delta\lambda^{\perp}$	Gorelik *et al.*[8])	0.08	0.09	1.8	2.1
n–D_2	$\Delta\lambda^{\perp}$	Gorelik *et al.*[8])	0.16	0.11	3.1	2.4
CH_4	$\frac{1}{2}(\Delta\lambda^{\perp}+\Delta\lambda^{//})$	Korving *et al.*[7])	2.7[5]	2.2	15.7	8.1
O_2	$\Delta\lambda^{\perp}$	Senftleben *et al.*[6])	see fig. 20			
	$\Delta\lambda^{//}$	Senftleben *et al.*[4])	10	8.3	14	14.0
	$\frac{1}{2}(\Delta\lambda^{\perp}+\Delta\lambda^{//})$	Korving *et al.*[7])	9.1	10.5	14	11.1

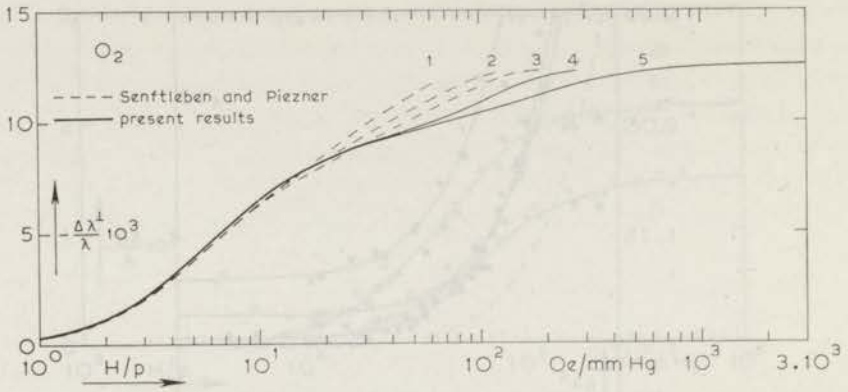

Fig. 20. Comparison between the results of Senftleben[6]) and the present measurements:

1. $p = 200$ mm Hg
2. $p = 100$ mm Hg
3. $p = 60$ mm Hg

} Senftleben

4. $p = 29.9$ mm Hg
5. $p = 7$–4 mm Hg

} present measurements.

The fact that the results of Korving *et al.*[7]) for $[\frac{1}{2}(\Delta\lambda^{\perp} + \Delta\lambda^{//})/\lambda]_{sat}$ are somewhat lower than ours (15–20%) for N_2, CO and O_2 may be attributable to the very complicated construction of the seals of their cell[16]). This does, however, not explain the discrepancies for CH_4. A comparison between the results of Senftleben[6]), who performed extensive measurements on $\Delta\lambda^{\perp}$ for O_2, and the present data is given in fig. 20, where smoothed curves taken from 3 pressure runs of fig. 18 are brought together with curves deduced from an analysis of Senftleben's work. A good agreement is found for the lower H/p region. In the higher H/p region deviations from the H/p law are seen both from Senftleben's data and from the present set. Allowing for these deviations from the H/p law, agreement between both sets of measurements is also found in the higher H/p region. Similar deviations from the H/p law were found in room temperature measurements on the influence of magnetic fields on the shear viscosity of O_2, as performed by Hulsman *et al.*[17]) over a wide pressure range (see also ref. 18). A brief discussion on the causes of this anomalous behaviour is given in chapter I; a thorough theoretical analysis is still in progress[19, 20]).

For a comparison with theory it must be recalled that the non-equilibrium distribution function is usually expanded in irreducible tensors made up of reduced velocity, $\boldsymbol{W}$, and angular momentum, $\boldsymbol{J}$ (see *e.g.* ref. 21). The term in this expansion which gives the major contribution in $\Delta\lambda^{\perp}$ and $\Delta\lambda^{//}$ is the $\boldsymbol{W}[\boldsymbol{J}]^{(2)}$ term, while the $\boldsymbol{WJ}$ term is expected to give a minor contribution, and even vanishes in the case of the existence of inverse collisions in classical mechanics. Furthermore, Hess and Köhler[22]) have shown that

for elastic collisions terms odd in $\boldsymbol{J}$ like $\boldsymbol{WJ}$ give a contribution to $\Delta\lambda/\lambda$ proportional only to the fourth power of the small non-sphericity of the molecular interaction, while terms even in $\boldsymbol{J}$ give contributions of the second power. The contribution arising from the $\boldsymbol{W}[\boldsymbol{J}]^{(2)}$ term alone has the following dependence on H/p:

$$-\left(\frac{\Delta\lambda^{\perp}}{\lambda}\right)=\psi_{12}\left\{\frac{\xi_{12}^2}{1+\xi_{12}^2}+2\frac{4\xi_{12}^2}{1+4\xi_{12}^2}\right\}, \tag{10a}$$

$$-\left(\frac{\Delta\lambda^{//}}{\lambda}\right)=\psi_{12}\left\{2\frac{\xi_{12}^2}{1+\xi_{12}^2}\right\}, \tag{10b}$$

where $\xi_{12}=c_{12}(g\mu_N\, kT/\hbar)(H/p)$ for diamagnetic molecules, g is the rotational g factor, μ_N the nuclear magneton, and ψ_{12} and c_{12} are related to collision integrals, which depend on the molecular interaction. The shape of the experimental curves agrees so well with these expressions (using ψ_{12} and c_{12} as adaptable parameters) that the deviations hardly exceed the measuring accuracy. This indicates, that the contributions of other terms than $\boldsymbol{W}[\boldsymbol{J}]^{(2)}$ are too small to be determined from the shape of the experimental curves alone. A more sensitive method to evaluate the importance of other terms in the distribution function is found by studying the ratio $(\Delta\lambda^{\perp}/\Delta\lambda^{//})_{\mathrm{sat}}$ which is, from an experimental point of view, the best determined quantity. Moreover, its value is rather sensitive to the presence of different expansion terms: a value of $(\Delta\lambda^{\perp}/\Delta\lambda^{//})_{\mathrm{sat}}=\frac{3}{2}$ follows from the $\boldsymbol{W}[\boldsymbol{J}]^{(2)}$ contribution (see eq. (10)), while this number increases rapidly with increasing influence of the $\boldsymbol{WJ}$ term (see fig. 1 in ref. 21). In fig. 19 a graph of the ratio $\Delta\lambda^{\perp}/\Delta\lambda^{//}$ *vs.* H/p as derived from eq. (10) is drawn at an arbitrary position along the H/p axis. As seen in this figure, the experimental results show small but significant deviations from this theoretical curve, based on the $\boldsymbol{W}[\boldsymbol{J}]^{(2)}$ term alone. For CO, which should be nearer than N_2 to having inverse collisions due to its loaded sphere character[21,23] – which reduces the influence of the $\boldsymbol{WJ}$ term –, the experimental results can be almost described by a pure $\boldsymbol{W}[\boldsymbol{J}]^{(2)}$ term. For HD this is even more the case (see table II). For the spherical top molecules CH_4, CD_4 and CF_4 significant deviations from the value $\frac{3}{2}$ are found (1.66, 1.60 and 1.53, respectively). If these molecules are described with the rough sphere interaction model[21,24] it is found that the $\boldsymbol{WJ}$ term can indeed contribute, leading to a value of about 1.6 for $(\Delta\lambda^{\perp}/\Delta\lambda^{//})_{\mathrm{sat}}$. This agreement is, however, rather fortuitous, since this theory has, as the authors of ref. 24 point out, only qualitative significance. This is supported by the facts, that this model predicts values for $\Delta\lambda/\lambda$ which are an order of magnitude larger than the observed values, and that, for the approximations made in ref. 24, the value of $(\Delta\lambda^{\perp}/\Delta\lambda^{//})_{\mathrm{sat}}$ increases with increasing reduced moment of inertia (*i.e.*, should be higher for CD_4 than for CH_4 and so forth) as opposed to the experimental results. Of all the investi-

gated gases there is only one, SF_6, which shows a ratio for $(\Delta\lambda^{\perp}/\Delta\lambda^{//})_{sat}$ which is smaller than $\frac{3}{2}$. This is in agreement with the work of Hess[25]) where the symmetry of octahedral molecules such as SF_6 and UF_6 is shown to result in terms in the distribution function (such as the $[\boldsymbol{W}]^{(3)}[\boldsymbol{J}]^{(4)}$ term), which are negligible for simpler molecules. This illustrates the relation between the symmetry of the molecular structure and the anisotropy of the distribution function in angular momentum space.

A quantitative interpretation of the magnitude of the effects, *i.e.*, $(\Delta\lambda^{\perp}/\lambda)_{sat}$ and $(\Delta\lambda^{//}/\lambda)_{sat}$ – or the value of ψ_{12} (see eq. (10)) – is not yet possible, as these are related through the off-diagonal collision integrals (see eq. (30) of ref. 21) to the non spherical part of the intermolecular potential. No calculations have yet been performed based on a realistic potential model. On the other hand, since the heat conductivity depends – as opposed to the viscosity[17,26]) – on more than one off-diagonal collision integral, it is not possible to use the experimental values to calculate the off-diagonal collision integrals. For the second quantity obtained from these experiments, *i.e.*, the value of $(H/p)_{\frac{1}{2}}$, the situation is much more favourable for two reasons. Firstly, $(H/p)_{\frac{1}{2}}$ is determined by only one (diagonal) collision integral, which can therefore be calculated from this experiment, and secondly because this collision integral is more amenable for theoretical calculations. The collision integral can best be obtained from the $\Delta\lambda^{\perp}$ curve, since a contribution of the very small $\boldsymbol{WJ}$ term on top of the dominant $\boldsymbol{W}[\boldsymbol{J}]^{(2)}$ term would be larger in the $\Delta\lambda^{//}$ than in the $\Delta\lambda^{\perp}$ curve. Using the expression for ξ_{12} as given in ref. 21 for the $\boldsymbol{W}[\boldsymbol{J}]^{(2)}$ contribution, it is found that

$$\left(\frac{H}{p}\right)^{\perp}_{\frac{1}{2}} = 0.6248\,\frac{\hbar}{|g|\,\mu_N kT}\,\frac{\langle[\boldsymbol{J}]^{(2)}_{ij}\boldsymbol{W}_k\mathfrak{R}_{\circ}\boldsymbol{W}_k[\boldsymbol{J}]^{(2)}_{ji}\rangle}{\frac{1}{4}\langle 4J^4 - 3J^2\rangle}, \tag{11}$$

where 0.6248 is the value of ξ_{12} for which the $\Delta\lambda^{\perp}/\lambda$ curve reaches half its saturation value (see eq. (10)), $\langle\ \ \rangle$ denotes an average over the equilibrium distribution function, and where one has to sum over equal indices and $\mathfrak{R}_{\circ} = -\mathcal{J}_0/n$, where n is the number density and $\mathcal{J}_0$ is the (dissipative) collision operator as defined in eq. (4) of ref. 21. In the same way as is done in chapter I the collision integral is given in the form of the quantity $\mathfrak{S}$ which is defined as

$$\mathfrak{S}\left(\begin{smallmatrix}1200\\1200\end{smallmatrix}\right) = \frac{\langle[\boldsymbol{J}]^{(2)}_{ij}\boldsymbol{W}_k\mathfrak{R}_{\circ}\boldsymbol{W}_k[\boldsymbol{J}]^{(2)}_{ji}\rangle}{\frac{1}{4}\langle 4J^4 - 3J^2\rangle}\,\frac{1}{\langle v_{rel}\rangle}, \tag{12}$$

where $\langle v_{rel}\rangle = \sqrt{8kT/\pi\mu}$ is the mean relative velocity with μ the reduced mass, and $\mathfrak{S}\left(\begin{smallmatrix}1200\\1200\end{smallmatrix}\right)$ has the dimension of a cross section*. The values for $\mathfrak{S}\left(\begin{smallmatrix}1200\\1200\end{smallmatrix}\right)$ obtained in this way from the experimental $(H/p)^{\perp}_{\frac{1}{2}}$ values are given

* The average in the numerator is such that if $\mathfrak{R}_0 = 1$, $\mathfrak{S}$ reduces to $1/\langle v_{rel}\rangle$.

TABLE IV

The values of $\Im\binom{1200}{1200}$ as calculated from the experimental values of $(H/p)_{\frac{1}{2}}^{\perp}$ according to eq. (12), and comparison with the elastic theory (see eq. (13)) ($T = 300$ K)

	$(H/p)_{\frac{1}{2},\mathrm{exp}}^{\perp}$	$\Im\binom{1200}{1200}$	$\frac{(H/p)_{\frac{1}{2},\mathrm{exp}}^{\perp}}{(H/p)_{\frac{1}{2}\mathrm{el.th.}}^{\perp}} = \frac{\text{experimental coll. integral}}{\text{theor. elast. coll. integral}}$
	(kOe/mm Hg)	Å^2	
N_2	4.8	48	1.8
CO	5.1[5]	49	1.8
HD	1.80	14	1.0
n–H_2	2.1	17	1.3
p–H_2	1.8	15	1.1
n–D_2	2.4	14	1.0
o–D_2	3.1	18	1.3
CH_4	6.8	57	1.8
CD_4	11.5	54	1.7
CF_4	43	84	1.7

in table IV. It is seen that the values found for $\Im\binom{1200}{1200}$ are about half the values which were found at 85 K from measurements of λ^{tr}. This temperature dependence of $\Im$ is consistent with that which is found for the ordinary viscosity and heat conductivity cross sections.

The second reason why the $(H/p)_{\frac{1}{2}}$ value is interesting lies in the fact that the diagonal collision integral can be easily determined for elastic collisions and so allows a measure for the inelasticity of the collisions. Making the assumption that J does not change upon collision (elastic model), the collision integral can be theoretically calculated, and one finds in that case (see *e.g.* ref. 27):

$$\left(\frac{H}{p}\right)_{\frac{1}{2},\mathrm{el.th.}}^{\perp} = 0.6248\,\frac{\hbar}{|g|\,\mu_N}\,\frac{8\pi^{\frac{1}{2}}\sigma^2\Omega^{(1,1)\star}}{3\sqrt{mkT}}, \tag{13}$$

where σ is the molecular diameter and $\Omega^{(1,1)\star}$ is the reduced omega integral (see ref. 28). Analogous to the procedure given in chapter I, the experimental value of $(H/p)_{\frac{1}{2}}^{\perp}$ is now compared to the one given in eq. (13). The ratio between the two, which is equal to the ratio of the realistic collision integral as derived from the experiment and the collision integral calculated in the elastic model, is given in table IV. The ratios obtained are nearly the same as those obtained at 85 K from measurements of λ^{tr}[1]), notwithstanding the fact that the collision integrals themselves vary by a factor of 2 over this temperature range, as discussed earlier; for most gases a ratio of approximately 2 is found. For the hydrogen isotopes where inelastic collisions only rarely occur, the elastic model should be quite satisfactory, and indeed a ratio of 1 is found within measuring accuracy.

1) Hermans, L. J. F., Schutte, A., Knaap, H. F. P. and Beenakker, J. J. M., Physica **46** (1970) 491. (Commun. Kamerlingh Onnes Lab., Leiden No. 375*b*).
2) Beenakker, J. J. M., Festkörperprobleme VIII, ed. O. Madelung, Vieweg Verlag (Braunschweig, 1968).
3) Beenakker, J. J. M. and McCourt, F. R., Ann. Rev. Phys. Chem. **21** (1970) (in print).
4) Senftleben, H. and Piezner, J., Ann. Physik **27** (1936) 108.
5) Michels, A. and Sengers, J. V., Physica **28** (1962) 1238.
6) Senftleben, H. and Piezner, J., Ann. Physik **27** (1936) 117
7) Korving, J., Honeywell, W. I., Bose, T. K. and Beenakker, J. J. M., Physica **36** (1967) 198 (Commun. Kamerlingh Onnes Lab., Leiden No. 357*c*).
8) Gorelik, L. L., Redkoborodyĭ, Yu. N. and Sinitsyn, V. V., Soviet Physics – JETP **21** (1965) 503.
9) Köhler, W. E., Z. Naturforsch., to be published.
10) Data Book (Thermophysical Properties Research Center, Purdue University, Lafayette, Indiana, 1966), Vol. 2.
11) Van Dael, W. and Cauwenbergh, H., Physica **40** (1968) 165.
12) Minter, C. C. and Schuldiner, S., J. Chem. Eng. Data **4** (1959) 223.
13) Hust, J. G. and Stewart, R. B., N.B.S. Report 8812 (1965).
14) Baker, C. E. and Brokaw, R. S., J. chem. Phys. **43** (1965) 3519.
15) Plank, R., Kältetechnik **10** (1958) 30.
16) Korving, J., private communication.
17) Hulsman, H. *et al.*, Physica, to be published.
18) Kikoin, I. K., Balashov, K. I., Lasarev, S. D. and Neushtadt, E., Phys. Letters **24A** (1967) 165.
19) Coope, J. A. R., McCourt, F. R. and Snider, R. F., J. chem. Phys., to be published.
20) Coope, J. A. R., Moraal, H. and Snider, R. F., J. chem. Phys., to be published.
21) Levi, A. C. and McCourt, F. R., Physica **38** (1968) 415 (Commun. Kamerlingh Onnes Lab., Leiden, Suppl. No. 126*a*).
22) Hess, S. and Köhler, W. E., Z. Naturforsch. **23a** (1968) 1903.
23) Dahler, J. S. and Sather, N. F., J. chem. Phys. **38** (1963) 2363.
24) McCourt, F. R., Knaap, H. F. P. and Moraal, H., Physica **43** (1969) 485 (Commun. Kamerlingh Onnes Lab., Leiden, Suppl. No. 127**c**).
25) Hess, S., Phys. Letters **28A** (1968) 87.
26) Korving, J., Physica **46** (1970) 619.
27) Knaap, H. F. P. and Beenakker, J. J. M., Physica **33** (1967) 643 (Commun. Kamerlingh Onnes Lab., Leiden, Suppl. No. 124*a*).
28) Hirschfelder, J. O., Curtiss, C. F. and Bird, R. B., The Molecular Theory of Gases and Liquids, John Wiley and Sons, Inc. (New York, 1954).

SAMENVATTING

In dit proefschrift worden experimenten beschreven over de invloed van magnetische velden op de warmtegeleiding, λ, van meeratomige gassen. Dit effect, dat direct in verband staat met de niet-bolvormigheid van dergelijke moleculen, blijkt twee aspecten te hebben. Enerzijds treedt er in de warmtegeleiding een verandering op, waarvan de grootte afhangt van de oriëntatie van het veld t.o.v. de warmtestroom: $\Delta\lambda^{//}$ en $\Delta\lambda^{\perp}$. Anderzijds treedt er onder invloed van een magnetisch veld een nieuwe (dwars-)warmtestroom op, die loodrecht staat op de aangelegde warmtestroom en het magneetveld, en die beschreven wordt door λ^{tr}. Een apparaat voor het meten van λ^{tr} wordt besproken in hoofdstuk I, en resultaten worden gegeven voor een aantal gassen bij temperaturen rond 85 K. Goede kwalitatieve overeenstemming wordt gevonden met de theorie, ontwikkeld volgens de methode van Chapman en Enskog voor een gas van roterende moleculen in een magnetisch veld. In hoofdstuk II worden resultaten van λ^{tr} gegeven voor de waterstofisotopen H_2, HD en D_2 in het temperatuurgebied van 20 tot 110 K. Deze gassen zijn in dit temperatuurgebied interessant omdat ze het mogelijk maken de invloed van de rotatietoestand op λ^{tr} te onderzoeken. Verder is een onderzoek van de waterstofisotopen van belang, omdat voor deze gassen de theoretische uitdrukkingen sterk kunnen worden vereenvoudigd, zodat een betere vergelijking tussen theorie en experiment mogelijk wordt. In hoofdstuk III worden metingen beschreven over de eerder genoemde veranderingen in de "gewone" warmtegeleiding, $\Delta\lambda^{//}$ en $\Delta\lambda^{\perp}$, die door een magnetisch veld worden teweeggebracht. De constructie van een vlakke platen-apparaat, waarin de warmtestroom overal dezelfde richting heeft, wordt besproken. Dit apparaat maakt het mogelijk om $\Delta\lambda^{//}$ en $\Delta\lambda^{\perp}$ te meten onder dezelfde omstandigheden, door de magneet te draaien rond het apparaat. Dit brengt met zich mee dat $\Delta\lambda^{\perp}/\Delta\lambda^{//}$ zeer nauwkeurig kan worden bepaald; deze grootheid geeft directe informatie over het mechanisme van de botsingen tussen twee roterende moleculen. Resultaten worden gegeven voor een tiental gassen bij kamertemperatuur.

Op verzoek van de faculteit der Wiskunde en Natuurwetenschappen volgen hier enige gegevens over mijn studie.

Na mijn Gymnasium-β opleiding van 1951 tot 1957 aan het Bernardinuscollege te Heerlen vervulde ik mijn militaire dienstplicht als officier bij de Koninklijke Luchtmacht. In 1959 begon ik mijn studie aan de Rijksuniversiteit te Leiden, waar ik in 1963 het candidaatsexamen aflegde in de Natuurkunde en Wiskunde met als bijvak Sterrenkunde. Sindsdien ben ik werkzaam op het Kamerlingh Onnes Laboratorium in de werkgroep Molecuulfysica onder leiding van Prof. Dr. J. J. M. Beenakker en Dr. H. F. P. Knaap. Aanvankelijk werkte ik mee aan een onderzoek naar de fasescheiding in vloeibare mengsels van neon en deuterium. Vervolgens heb ik een onderzoek verricht naar het verschil in polariseerbaarheid tussen waterstofisotopen. Vanaf 1964 ben ik assistent op het natuurkundig practicum voor prekandidaten. Medio 1965 begon ik aan onderzoekingen op het gebied van de invloed van magnetische velden op de warmtegeleiding van meeratomige gassen. In 1966 legde ik het doctoraalexamen Natuurkunde af, en sindsdien ben ik als wetenschappelijk medewerker in dienst van de Stichting voor Fundamenteel Onderzoek der Materie (F.O.M.).

In 1964 werkte ik gedurende enkele maanden in het "Instituut voor Lage Temperaturen en Technische Fysica" te Leuven, en in 1967 gedurende een maand aan de "Istituto di Fisica" van de Universiteit te Genua.

Een belangrijk aandeel in het onderzoek, dat in dit proefschrift wordt beschreven, hadden de heren drs. A Schutte en drs. J. M. Koks, terwijl ik in verschillende stadia van het experimentele werk geassisteerd werd door de heren drs. J. J. de Groot, drs. P. H. Fortuin, R. W. C. Brom, drs. G. van der Hoek en A. F. Hengeveld.

Dat een onderzoek is opgezet naar het bestaan van dwars-warmtetransport in een magnetisch veld is in belangrijke mate te danken aan de stimulerende invloed van Prof. Dr. P. Mazur. Veel steun op theoretisch gebied heb ik ondervonden van de samenwerking met Dr. F. R. McCourt van de Universiteit van Waterloo, Canada, Dr. A. C. Levi van de Universi-

teit van Genua, en Dr. S. Hess en Dr. W. E. Köhler van de Universiteit van Erlangen–Nürnberg. De constructie van de beide apparaten, nodig voor het onderzoek, werd op zeer bekwame wijze uitgevoerd door de heren J. M. Verbeek en P. Zwanenburg. Een aantal onmisbare technische voorzieningen kwamen tot stand dank zij de inspanningen van verscheidene leden van de vaste staf van het Kamerlingh Onnes Laboratorium, met name de heren J. Turenhout, J. Dunsbergen en T. A. van der Heijden. De heer W. F. Tegelaar verzorgde de tekeningen van dit proefschrift, terwijl mej. S. M. J. Ginjaar en mej. A. M. Aschoff zorgden voor het ontcijferen en typen van het manuscript. De Engelse tekst werd gecorrigeerd door Dr. F. R. McCourt en Dr. V. G. Cooper.